

SRT1720 improves survival and healthspan of obese mice

Robin K. Minor¹, Joseph A. Baur², Ana P. Gomes³, Theresa M. Ward¹, Anna Csiszar⁴, Evi M. Mercken¹, Kotb Abdelmohsen⁵, Yu-Kyong Shin⁶, Carles Canto⁷, Morten Scheibye-Knudsen⁸, Melissa Krawczyk⁹, Pablo M. Irusta^{1,10}, Basil P. Hubbard³, Yongqing Zhang¹¹, Elin Lehrmann¹¹, Alexa A. White⁶, Nathan L. Price³, William R. Swindell¹², Kevin J. Pearson^{1,13}, Kevin G. Becker¹¹, Vilhelm A. Bohr⁸, Myriam Gorospe⁵, Josephine M. Egan⁶, Mark I. Talan⁹, Johan Auwerx⁷, Christoph H. Westphal¹⁴, James L. Ellis¹⁴, Zoltan Ungvari⁴, George P. Vlasuk¹⁴, Peter J. Elliott¹⁴, David A. Sinclair³ & Rafael de Cabo^{1*}

*To whom correspondence should be addressed. E-mail: decabora@mail.nih.gov

SI includes:

Supplementary Methods
Supplementary Figures 1-7
Supplementary Tables 1-4

SUPPLEMENTARY METHODS

Echocardiography

Echocardiography was conducted under 2% Isoflurane anesthesia delivered via nose cone using the VisualSonics 770 imaging system with a 30 MHz probe (Toronto, Canada). Briefly, parasternal short axis views were obtained at the midpapillary muscle level. Measurements were made from the short axis M-mode from digital images captured on cineloop using the leading edge method. End diastolic (EDV) and end systolic volume (ESV) measurements were calculated using a modified Simpson's method. Ejection Fraction (EF) was derived as $EF = (EDV - ESV)/EDV \times 100$. All measurements were averaged over three to five consecutive cycles. The reproducibility of measurements was assessed in two sets of baseline measurements in 10 randomly selected mice and the repeated measure variability did not exceed 5%. The ECG recorded during ~10 min of each Echo was evaluated to detect and record rhythm disturbances.

Metabolic and physical activity

Mouse metabolic rate was assessed by indirect calorimetry in open-circuit oxymax chambers using the Comprehensive Lab Animal Monitoring System (CLAMS; Columbus Instruments, Columbus, OH). Mice were housed singly with water and food available *ad libitum* and maintained at ~24°C under a 12:12-h light-dark cycle (light period 0600-1800). All mice were acclimatized to monitoring cages for 3-6 h prior to the recording began. Sample air was passed through an oxygen (O_2) sensor for determination of O_2 content. O_2 consumption was determined by measuring oxygen concentration in air entering the chamber compared

with air leaving the chamber. The sensor was calibrated against a standard gas mix containing defined quantities of O₂, CO₂, and N₂. Constant airflow (0.6 L/min) was drawn through the chamber and monitored by a mass-sensitive flow meter. The concentrations of oxygen and carbon dioxide were monitored at the inlet and outlet of the sealed chambers to calculate oxygen consumption. Each chamber was measured for 30 s at 30-min intervals and data were recorded for 60 h total. Movement (both horizontal and vertical) was also monitored. The system has beams 0.5 inches apart on the horizontal plane providing a high-resolution grid covering the XY-planes and the software provides counts of beam breaks by the mouse in 30-s epochs.

Inclined Screen

Mice were placed in a tilted, open field (55 cm² surface area constructed from a 0.6 cm² wire mesh grid with black sides extending 15 cm above the grid) and movement was recorded for 300 s using Field 2020 tracking software from HVS Image (Buckingham, UK). Results were averaged for total distance traveled for each mouse.

Quantitative Real-Time PCR

Total RNA was isolated with the Mini RNA Isolation Kit (Zymo Research, Orange, CA) and was reverse transcribed using Superscript II RT (Invitrogen, Carlsbad, CA). Real time PCR was used to analyze mRNA expression ($n = 5-6$ for each group) using the Mx3000 (Stratagene, La Jolla, CA). Amplification efficiencies were determined using a dilution series of a standard vascular sample. Quantification was performed using the efficiency-corrected ΔΔCq method.

The relative quantities of the reference genes hypoxanthine guanine phosphoribosyl transferase (HPRT), ubiquitin C (UBC), tyrosine 3-monoxygenase / tryptophan 5-monoxygenase activation protein, zeta polypeptide (YWHAZ) and/or β-actin were determined and a normalization factor was calculated based on their geometric mean for internal normalization. The oligonucleotides used for quantitative real-time RT-PCR are listed in supplementary table 3. Fidelity of the PCR reaction was determined by melting temperature analysis and visualization of product on a 2% agarose gel.

Apoptosis and inflammatory measures

Tissue samples were lysed and cytoplasmic histone-associated DNA fragments, which indicate apoptotic cell death, were quantified by the Cell Death Detection ELISA-Plus kit (Roche Diagnostics Corporation, Indianapolis, IN) according to the manufacturer's protocol. Results are reported as arbitrary optical density (O.D.) units normalized to protein concentration.

Caspase 3/7 activities in tissue lysates were measured using the Caspase-Glo 3/7 assay kit (Promega, Madison, WI) according to the manufacturer's instructions. Briefly, in 96-well plates 50 µl of sample was mixed gently for 30 s with 50 µl Caspase-Glo 3/7 reagent and incubated for 2 h at room temperature. Lysis buffer with reagent alone served as a blank. Luminescence of the samples was measured using an Infinite M200 plate reader (Tecan, Research Triangle Park, NC). Luminescent intensity values were normalized to the sample protein concentration.

Levels of isoprostanes in the hearts and livers were assessed using the Isoprostane Oxidative Stress Assay Kit B (Enzo Life Sciences International, Inc., Plymouth Meeting, PA) according to the manufacturer's protocol.

Circulatory levels of inflammatory markers (TNF- α , IL-6, MCP-1 and leptin) were measured with the Mouse Serum Adipokine Panel from Milliplex (Millipore, Billerica, MA) according to the manufacturer's protocol.

Microarray

RNA was extracted from liver samples using Trizol Reagent following the manufacturer's instructions (Invitrogen, Carlsbad, CA) and hybridized to MouseRef-8 v2 Expression beadchips (Illumina, San Diego, CA). Microarray experiments were performed using the MouseRef-8 v2.0 Expression BeadChips (Illumina, San Diego, CA) following protocols listed on the Gene Expression and Genomics Unit of the NIA (<http://www.grc.nia.nih.gov/branches/rrb/dna/index/protocols.htm>). Raw data were subjected to Z normalization to ensure compatibility using the formula:

$$Z\text{score}_{\text{gene}} = \frac{\ln(\text{signal})_{\text{gene}} - \overline{\ln(\text{signal})_{\text{gene}}}}{\sigma(\ln(\text{signal}))_{\text{gene}}}$$

where \ln is natural logarithm, $\overline{\ln(\text{signal})_{\text{gene}}}$ is the average over all genes of an array, and $\sigma(\ln(\text{signal}))_{\text{gene}}$ is the standard deviation over all genes of an array. The Z ratio (between treatment A and control B) is given by:

$$Zratio(A - B) = \frac{\overline{Zscore(A)} - \overline{Zscore(B)}}{\sigma_{(A-B)}}$$

Where $\overline{Zscore(A)}$ is the mean value of group A's (treatment) zscores and $\overline{Zscore(B)}$ is the mean value of group B's (control) zscores. $\sigma_{(A-B)}$ is the standard derivative of group A versus group B. For group comparisons z-tests or unpaired t-tests were employed for the two groups of zscores for each probe/gene. Individual genes with $|Zratio(A-B)| \geq 1.5$, P value $(A-B) \leq 0.05$, false discovery rate $fdr (A-B) \leq 0.30$, and average zscore intensity of the comparing group $(A,B) > 0$ were considered significantly changed.

For verification of specific results we performed reverse transcription (RT) using random hexamers and SSII reverse transcriptase (Invitrogen), after which real-time quantitative (q)PCR analysis was performed using gene-specific primer pairs (Supplementary Table 3).

For parametric analysis of gene set enrichment (PAGE), a set of 1687 pathways was obtained from http://www.broad.mit.edu/gsea/msigdb/msigdb_index.html (C2 collection). Our expression data was tested for gene set enrichment using the PAGE method as previously described¹. Briefly, for each pathway under each pair of conditions, a Z score was computed as $[Z(\text{pathway}) = (sm\ mu) * \text{pow}(m, 0.5) / \delta]$, where μ = mean Z score of all gene symbols on the microarray, δ = standard deviation of Z scores of all gene symbols on the microarray, sm = mean Z score of gene symbols comprising one pathway present on the microarray, and m = number of gene symbols in a pathway present on the microarray. For each $Z(\text{pathway})$ a P value was also computed in JMP 6.0 to test for the significance of the Z score obtained. These

tools are part of DIANE 1.0 and are available at

http://www.grc.nia.nih.gov/branches/rrb/dna/diane_software.pdf.

We compared expression profiles between SRT1720-treated (cDNA hybridized to the Illumina MouseRef-8 v2.0 expression beadchip with 25697 transcripts) and resveratrol-treated (cDNA hybridized to the Illumina mouseRef-8 v1.1 expression beadchip with 24613 transcripts) mice, based upon 16075 transcripts that are shared between the Illumina MouseRef-8 v2.0 and Illumina mouseRef-8 v1.1 platforms. Expression data from both platforms was normalized using Z-score transformation and the significance of treatment differences was evaluated using the Z-ratio test method that has been previously described². Based upon this method, a total of 251, 281, 67 and 223 transcripts were significantly up regulated by 30 mg/kg SRT1720, 100 mg/kg SRT1720, low resveratrol and high resveratrol, respectively ($P < 0.05$). Likewise, a total of 310, 309, 96 and 239 transcripts were significantly down regulated by 30 mg/kg SRT1720, 100 mg/kg SRT1720, low resveratrol and high resveratrol, respectively ($P < 0.05$).

Some differentially expressed transcripts were not included among the 16075 transcripts that are shared between the Illumina MouseRef-8 v2.0 and Illumina mouseRef-8 v1.1 beadchips. With respect to such transcripts, it was not possible to make comparisons between the effects of SRT1720 and resveratrol. Among the 16075 transcripts that were comparable between platforms, a total of 168, 181, 58 and 181 were up regulated by 30 mg/kg SRT1720, 100 mg/kg SRT1720, low resveratrol and high resveratrol, respectively ($P < 0.05$). Likewise, among these 16075 transcripts, 184, 181, 70 and 163 were down regulated by 30 mg/kg SRT1720, 100 mg/kg SRT1720, low resveratrol and high resveratrol, respectively ($P < 0.05$).

The association between resveratrol and SRT1720 was evaluated based upon four pairwise comparisons of transcriptional patterns (low resveratrol vs. 30 mg/kg SRT1720; high resveratrol vs. 30 mg/kg SRT1720; low resveratrol vs. 100 mg/kg SRT1720; high resveratrol vs. 100 mg/kg SRT1720). For each comparison, differential expression signatures corresponding to the respective effects of resveratrol and SRT1720 were constructed, and based upon cross-tabulation of these signatures, we evaluated evidence for a non-random association between SRT1720- and resveratrol-associated differential expression patterns (Supplementary Fig. 5).

Cell culture, survival and mitochondrial biogenesis

Primary MEFs in which SIRT1 had been inactivated via exon deletion were a kind gift from Raul Mostoslavsky. MEFs were immortalized in culture using a standard 3T3 protocol³. Immortalized MEFs were maintained in DMEM medium (4.5g glucose / L) supplemented with 10% fetal bovine serum (FBS) and 100 µg/ml penicillin/streptomycin and cells were not grown to higher than 80% confluence.

For SRT1720 treatments, the compound was dissolved in DMSO and the final concentration of DMSO was 0.6% or less for all treatments. The MTT assay was used for cell survival assessment as a putative marker of mitochondrial activity based on the reduction of the tetrazolium salt MTT (3-[4,5-dimethylthiazol-2-yl]-2,5-diphenyltetrazoliumbromide) into a blue formazan product by the mitochondrial enzyme succinate dehydrogenase⁴. MEFs were pretreated with SRT1720 for 24h and 500 µM H₂O₂ was then added to the cells. After incubation for 24h at 37°C, cell survival was determined.

***In vitro* Sirt1 deacetylase activity**

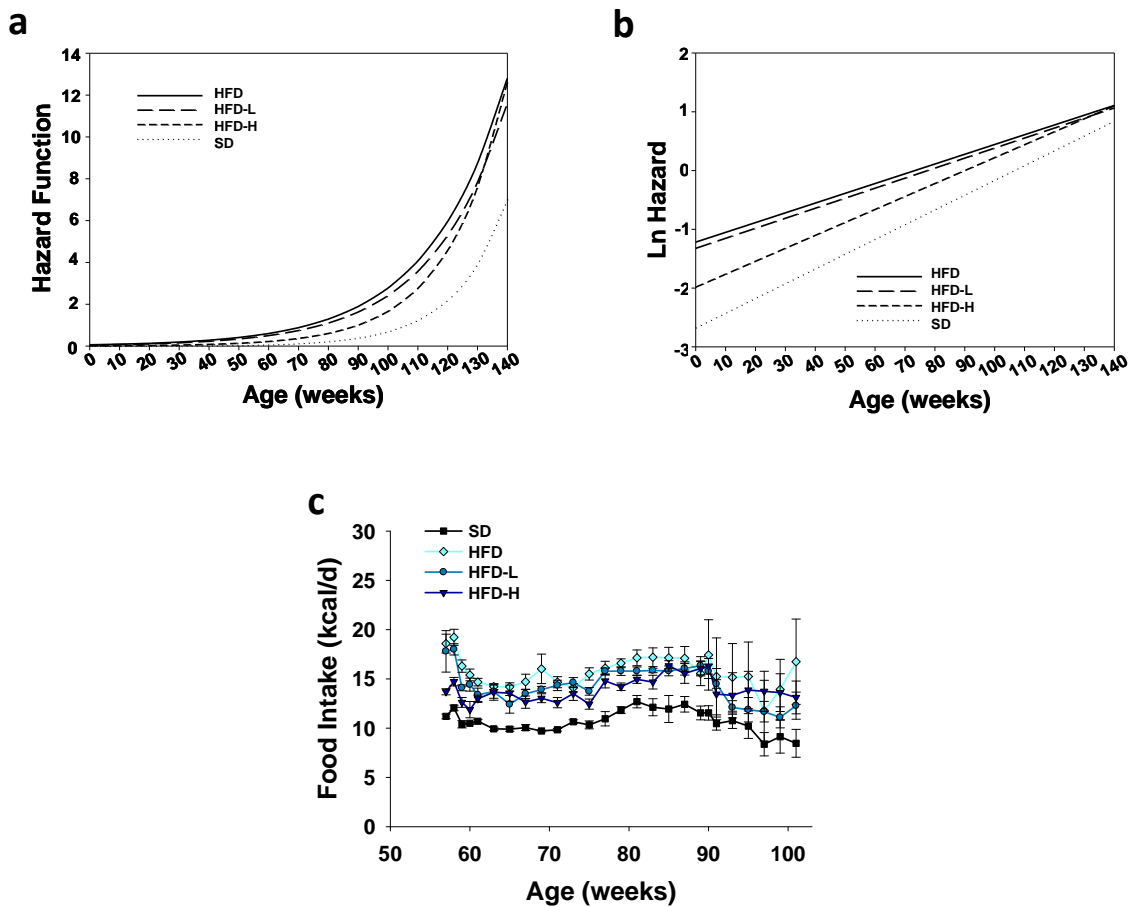
Recombinant full-length human His-tagged Sirt1 was produced in BL21(DE3) pLysS bacteria, and purified as previously described for dSir2⁵. The Fluor de Lys deacetylase assay (Enzo Life Sciences International, Plymouth Meeting, PA) was performed in accordance with the manufacturers' instructions. The final B-NAD⁺ concentration in each reaction was 60 µM, and the final FdL-p53 substrate concentration used was 30 µM. 5 µg of recombinant His-hSirt1 was added to each reaction, and developer was added following a 1 h incubation at 37°C.

Western blotting and p53 deacetylation

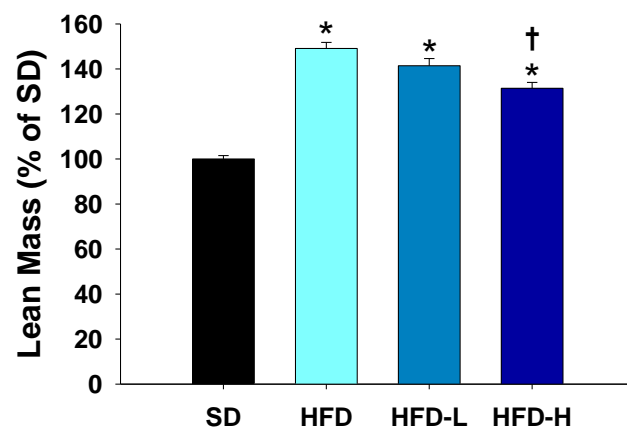
SIRT1 WT and KO MEFs were treated for 4 h with SRT1720 (3 µM) and whole-cell lysates prepared. Western blot analysis was performed using antibodies that recognized SIRT1 (Santa Cruz Biotechnology, Santa Cruz, CA), acetyl p53 (Cell Signaling), p53 (Calbiochem, San Diego, CA) or GAPDH (Santa Cruz). Following incubation with the appropriate secondary antibodies (Amersham (GE Healthcare), Piscataway, NJ), signals were detected by using enhanced luminescence (Amersham).

SUPPLEMENTARY REFERENCES

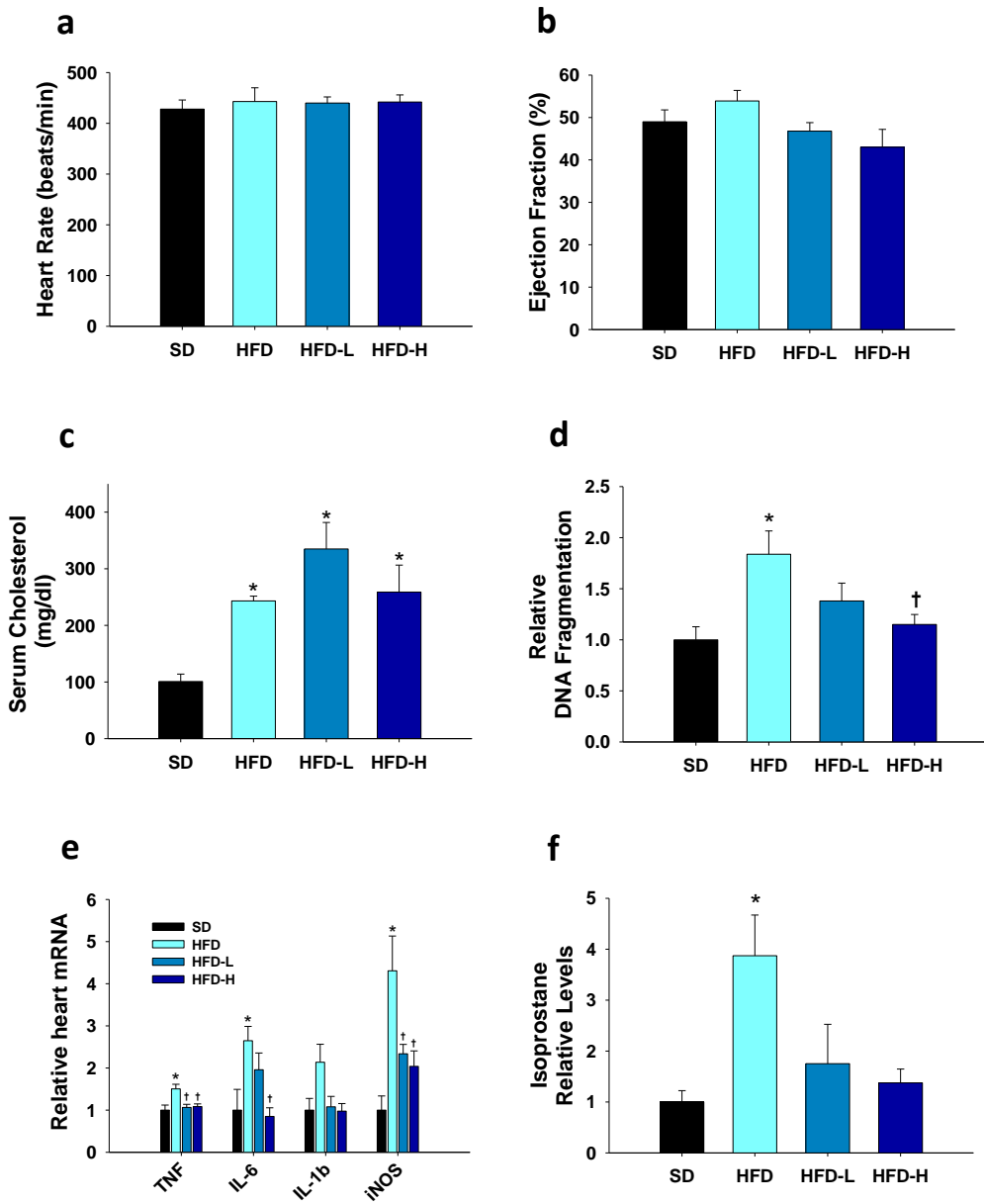
1. Kim, S. Y. & Volsky, D. J. PAGE: parametric analysis of gene set enrichment. *BMC Bioinformatics* **6**, 144 (2005).
2. Cheadle, C., Vawter, M. P., Freed, W. J. & Becker, K. G. Analysis of Microarray Data Using Z Score Transformation *J. Mol. Diagn.* **5**, 73-81 (2003).
3. Todaro, G. J. & Green, H. Quantitative studies of the growth of mouse embryo cells in culture and their development into established lines. *J. Cell Biol.* **17**, 299-313 (1963).
4. Mosmann, T. Rapid colorimetric assay for cellular growth and survival: application to proliferation and cytotoxicity assays. *J. Immunol. Methods* **65**, 55-63 (1983).
5. Maftah, A., Petit, J. M., Ratinaud, M. H. & Julien, R. 10-N nonyl-acridine orange: a fluorescent probe which stains mitochondria independently of their energetic state. *Biochem. Biophys. Res. Commun.* **164**, 185-190 (1989).
6. Picard, F. et al. Sirt1 promotes fat mobilization in white adipocytes by repressing PPAR-gamma. *Nature* **429**, 771-776 (2004).
7. Banks, A. S. et al. SirT1 gain of function increases energy efficiency and prevents diabetes in mice. *Cell Metab.* **8**, 333-341 (2008).
8. Pfluger, P. T., Herranz, D., Velasco-Miguel, S., Serrano, M. & Tschoep M. H. Sirt1 protects against high-fat diet-induced metabolic damage. *Proc. Natl. Acad. Sci. USA* **105**, 9793-9798 (2008).
9. Escande, C. et al. Deleted in breast cancer-1 regulates SIRT1 activity and contributes to high-fat diet-induced liver steatosis in mice. *J. Clin. Invest.* **120**, 545-558 (2010).



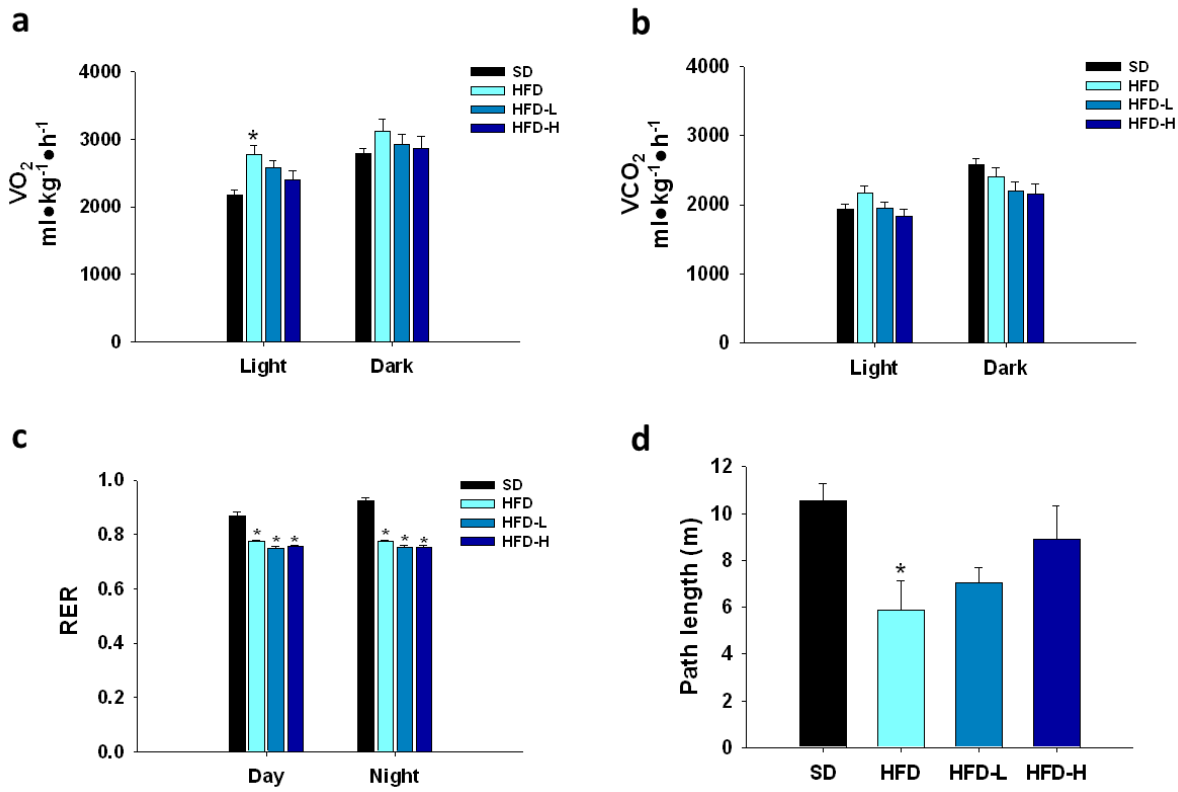
Supplementary Figure 1 | Mortality rates and food consumption in the diet groups. (a) Hazard function curves over time and (b) the natural log of the hazard functions show that the curves of the HFD group are the highest at younger ages (up ~ 120 weeks) where the HFD-L and HFD-H groups are proportionately skewed towards the curves of the SD group. (c) Caloric intake is increased in the groups on the high fat diet throughout the duration of the feeding study ($n \leq 12$ with 3 cages of 4 mice each at onset of diets). Data are represented as the mean \pm SEM.



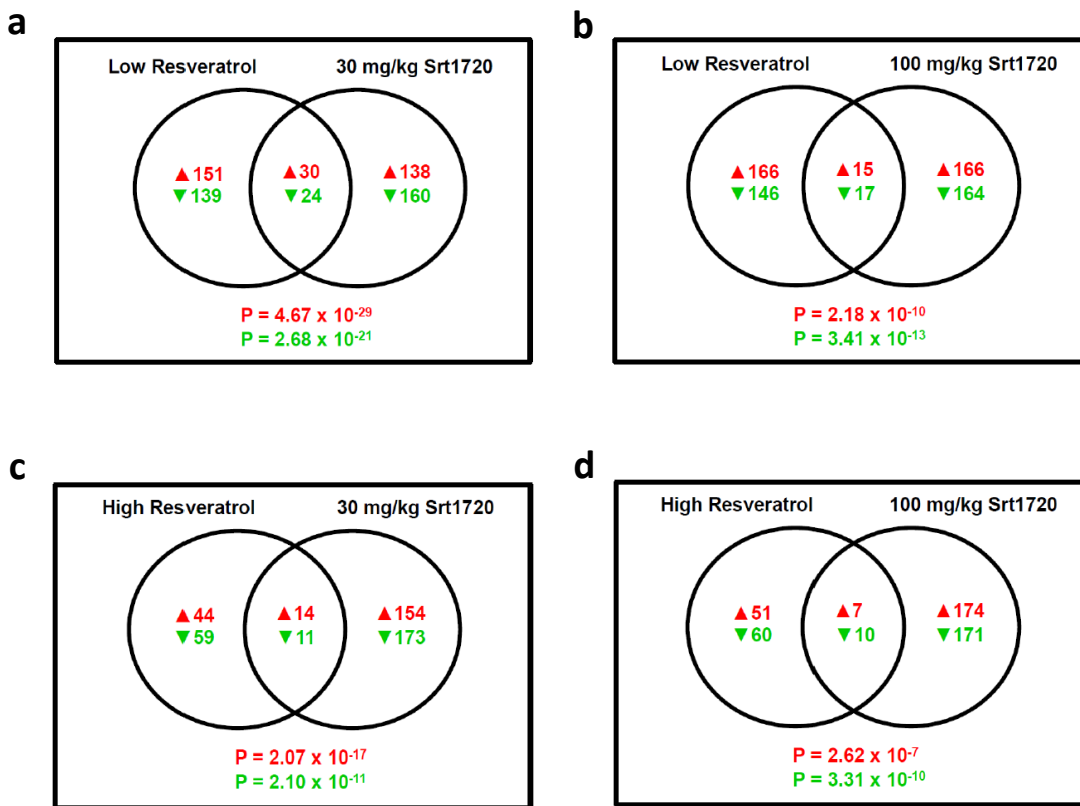
Supplementary Figure 2 | Lean mass.



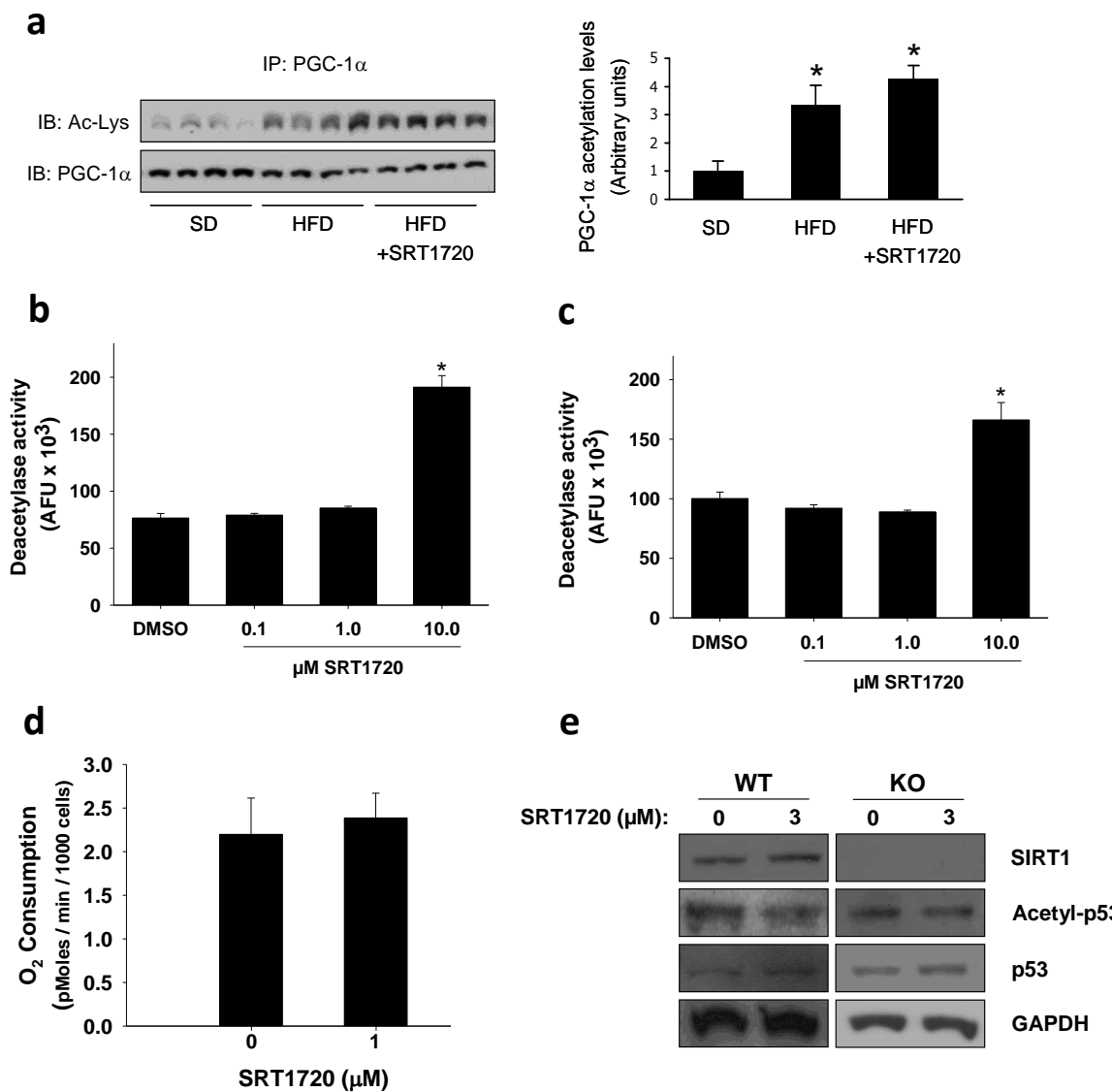
Supplementary Figure 3 | Cardiovascular functional and molecular changes induced by SRT1720 treatment in the diet. As measured by echocardiogram neither heart rate (**a**) nor ejection fraction (**b**) are affected by diet or treatment ($n = 10$; age = 119 wks; diet = 63 wks). Total cholesterol (**c**) is elevated in all high fat groups compared with SD ($n = 6$; age = 82 wks; diet = 26 wks). DNA fragmentation (**d**), an indication of cellular apoptosis, is elevated in HFD mice only and is significantly lowered in HFD-H compared with HFD. The increase in transcript levels of inflammatory markers (**e**) by HFD is attenuated by treatment with SRT1720. Isoprostanate levels (**f**), markers of oxidative stress, are increased in the HFD group compared with SD but not in the groups supplemented with SRT1720 ($n = 6$; age = 82 wks; diet = 26 wks). Data are represented as the mean \pm SEM. * $P < 0.0083$ from SD; † $P < 0.0083$ from HFD.



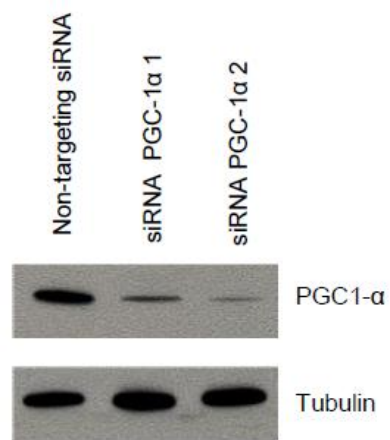
Supplementary Figure 4 | Metabolic and physical activity response to SRT1720. Oxygen consumption (a) but not carbon dioxide output (b) is dysregulated in the HFD mice during the light cycle ($n = 14$ (SD), 12 (HFD), 10 (HFD-L), 14 (HFD-H); age = 122 wks; diet = 66 wks). The respiratory exchange ratio (RER) is reduced in all HFD groups compared with SD (c). Reduced locomotor activity associated with the HFD is prevented by SRT1720 (d) in the inclined screen test ($n = 9$; age = 69 wks; diet = 13 wks). Data are represented as the mean \pm SEM. * $P < 0.0083$ from SD.



Supplementary Figure 5 | Overlap of the effects of SRT1720 and resveratrol in the livers of mice. Resveratrol and SRT1720 signatures in gene upregulation and gene downregulation are represented in Venn diagrams with overlapping gene effects represented in the junctions. Red stands for the number of upregulated transcripts and green stands for the number of downregulated transcripts. P-values listed in each section are generated from hypergeometric tests of the overlaps.



Supplementary Figure 6 | Effects of SRT1720 on acetylation levels in muscle and MEFs and on oxygen consumption *in vitro*. Relative PGC-1 α acetylation in the muscle (a) was analyzed by immunoprecipitation from nuclear extracts followed by an immunoblot against acetylated lysine residues ($n = 8$; age = 40 weeks; diet = 12 weeks). Data are represented as the mean \pm SEM. * $P < 0.0083$ from SD. SRT1720 promotes Sirt1 deacetylase activity *in vitro* towards both p53 (b) and H4K16 (c). Data are represented as the mean \pm SEM. * $P < 0.05$ from DMSO. SRT1720 does not increase basal respiration in cultured MEFs (d). Immunoblots of MEFs from SIRT1 wild type (WT) and SIRT1 knockout (KO) mice (e) show a greater reduction of acetylated p53 after SRT1720 treatment in the WT MEFs (50% deacetylation normalized to GAPDH) compared with KO MEFs (20%), indicating SRT1720 promotes Sirt1 deacetylase activity.



Supplementary Figure 7 | Extent of PGC-1 α knockdown by siRNA transfection. Relative tubulin and PGC-1 α expression following treatment with non-targeting and PGC-1 α specific siRNAs.

Supplementary Table 1 | Survival data.

ALL MICE BORN 10.25.2006															
Group	Mouse #	Death Date	Age (wk)	Group	Mouse #	Death Date	Age (wk)	Group	Mouse #	Death Date	Age (wk)	Group	Mouse #	Death Date	Age (wk)
SD	54	12.21.07-F	60	HFD	351	1.22.08-T	64	HFD-L	505	1.05.08-Sa	62	HFD-H	580	2.13.08-W	67
SD	20	3.11.08-T	71	HFD	369	1.23.08-W	64	HFD-L	435	1.15.08-T	63	HFD-H	528	3.11.08-T	71
SD	3	3.13.08-R	72	HFD	373	1.23.08-W	64	HFD-L	488	1.20.08-Su	64	HFD-H	573	3.25.07-T	73
SD	49	4.06.09-Su	75	HFD	396	1.23.08-W	64	HFD-L	466	1.22.08-T	64	HFD-H	565	3.31.08-M	74
SD	73	5.14.08-W	80	HFD	323	1.29.07-T	65	HFD-L	449	1.24.08-R	65	HFD-H	554	5.22.08-R	82
SD	7	5.27.08-T	82	HFD	318	2.01.08-F	66	HFD-L	476	1.28.08-M	65	HFD-H	587	5.22.08-R	82
SD	8	5.27.08-T	82	HFD	322	2.06.08-W	66	HFD-L	448	2.01.08-F	66	HFD-H	553	5.24.08-Sa	82
SD	9	5.27.08-T	82	HFD	368	2.10.08-Su	67	HFD-L	484	2.01.08-F	66	HFD-H	556	5.27.08-T	82
SD	67	5.27.08-T	82	HFD	406	2.10.08-Su	67	HFD-L	469	2.04.08-M	66	HFD-H	557	5.27.08-T	82
SD	68	5.27.08-T	82	HFD	361	2.18.08-M	68	HFD-L	438	2.10.08-Su	67	HFD-H	558	5.27.08-T	82
SD	69	5.27.08-T	82	HFD	411	2.20.08-W	68	HFD-L	447	2.10.08-Su	67	HFD-H	568	5.27.08-T	82
SD	42	7.08.08-T	88	HFD	359	2.20.08-W	68	HFD-L	463	2.15.08-F	68	HFD-H	569	5.27.08-T	82
SD	25	7.11.08-F	89	HFD	405	2.20.08-W	68	HFD-L	426	2.19.08-T	68	HFD-H	570	5.27.08-T	82
SD	81	7.23.08-W	90	HFD	400	2.25.08-M	69	HFD-L	511	2.26.08-T	69	HFD-H	574	6.03.08-T	83
SD	64	7.26.08-Sa	91	HFD	372	3.03.08-M	70	HFD-L	517	3.01.08-Sa	70	HFD-H	551	6.26.08-R	87
SD	46	8.13.08-W	93	HFD	404	3.06.08-R	71	HFD-L	518	3.02.08-Su	70	HFD-H	578	7.01.08-T	87
SD	13	8.25.08-M	95	HFD	327	3.07.08-F	71	HFD-L	501	3.06.08-R	71	HFD-H	592	7.13.08-Su	89
SD	26	8.30.08-Sa	96	HFD	334	3.13.08-R	72	HFD-L	462	3.07.08-F	71	HFD-H	526	7.23.08-W	90
SD	2	8.31.08-Su	96	HFD	388	3.14.08-F	72	HFD-L	498	3.13.08-R	72	HFD-H	597	7.26.08-Sa	91
SD	6	9.24.08-W	99	HFD	335	3.19.08-W	72	HFD-L	439	3.14.08-F	72	HFD-H	577	8.02.08-Sa	92
SD	60	9.24.08-W	99	HFD	357	3.19.08-W	72	HFD-L	443	3.20.08-R	73	HFD-H	530	8.15.08-F	94
SD	100	10.20.08-M	103	HFD	398	3.19.08-W	72	HFD-L	512	4.17.08-R	77	HFD-H	591	8.15.08-F	94
SD	102	10.22.08-W	103	HFD	420	3.19.08-W	72	HFD-L	490	4.20.08-Su	77	HFD-H	606	8.21.08-R	95
SD	22	10.27.08-M	104	HFD	326	3.23.08-Su	73	HFD-L	456	4.21.08-M	77	HFD-H	546	8.27.08-W	95
SD	98	11.01.08-Sa	105	HFD	399	3.24.08-M	73	HFD-L	491	5.01.08-R	79	HFD-H	542	8.30.08-Sa	96
SD	71	11.12.08-W	106	HFD	418	3.29.08-Sa	74	HFD-L	481	5.05.08-M	79	HFD-H	613	9.02.08-T	96
SD	92	11.12.08-W	106	HFD	414	3.31.08-M	74	HFD-L	500	5.09.08-F	80	HFD-H	594	9.09.08-T	97
SD	14	11.13.08-R	107	HFD	391	4.07.08-M	75	HFD-L	487	5.14.08-W	80	HFD-H	626	9.11.08-R	98
SD	53	11.17.08-M	107	HFD	397	4.07.08-M	75	HFD-L	506	5.23.08-F	82	HFD-H	564	9.20.08-Sa	99
SD	34	11.19.08-W	107	HFD	332	4.24.08-R	78	HFD-L	514	5.25.08-Su	82	HFD-H	611	9.27.08-Sa	100
SD	21	11.20.08-R	108	HFD	957	4.25.08-F	78	HFD-L	464	5.27.08-T	82	HFD-H	538	10.02.08-R	101
SD	59	11.21.08-F	108	HFD	331	4.29.08-T	78	HFD-L	465	5.27.08-T	82	HFD-H	539	10.03.08-F	101
SD	41	12.01.08-M	109	HFD	384	5.05.08-M	79	HFD-L	486	5.27.08-T	82	HFD-H	560	10.14.08-T	102
SD	48	12.01.08-M	109	HFD	402	5.05.08-M	79	HFD-L	489	5.27.08-T	82	HFD-H	552	10.22.08-W	103
SD	11	12.03.08-W	109	HFD	381	5.19.08-M	81	HFD-L	507	5.27.08-T	82	HFD-H	549	10.31.08-F	105
SD	83	12.03.08-W	109	HFD	377	5.23.08-F	82	HFD-L	519	5.27.08-T	82	HFD-H	531	11.03.08-M	106
SD	89	12.03.08-W	109	HFD	378	5.23.08-F	82	HFD-L	483	5.29.08-R	83	HFD-H	534	11.18.08-T	107
SD	52	12.06.08-Sa	110	HFD	379	5.24.08-Sa	82	HFD-L	473	5.29.08-R	83	HFD-H	615	11.18.08-T	107
SD	76	12.15.08-M	111	HFD	380	5.25.08-Su	82	HFD-L	494	6.04.08-W	83	HFD-H	536	11.20.08-R	108
SD	70	12.17.08-W	111	HFD	324	5.27.08-T	82	HFD-L	513	7.11.08-F	89	HFD-H	577	11.21.08-F	108
SD	1	01.18.09-Su	116	HFD	362	5.27.08-T	82	HFD-L	515	7.18.08-F	90	HFD-H	562	11.26.08-W	108
SD	93	01.29.09-R	118	HFD	383	5.27.08-T	82	HFD-L	470	7.24.08-R	91	HFD-H	614	11.28.08-F	109
SD	85	01.30.09-F	118	HFD	385	5.27.08-T	82	HFD-L	433	7.31.08-R	92	HFD-H	609	11.29.08-Sa	109
SD	99	02.03.09-T	118	HFD	387	5.27.08-T	82	HFD-L	497	8.02.08-Sa	92	HFD-H	571	12.03.08-W	109
SD	82	02.04.09-W	118	HFD	401	5.27.08-T	82	HFD-L	468	8.13.08-W	93	HFD-H	599	12.03.08-W	109
SD	84	02.04.09-W	118	HFD	325	6.04.08-W	83	HFD-L	428	8.26.08-T	95	HFD-H	603	12.03.08-W	109
SD	19	02.05.09-R	119	HFD	343	6.04.08-W	83	HFD-L	499	9.09.08-T	97	HFD-H	584	12.07.08-Su	110
SD	86	02.05.09-R	119	HFD	347	6.05.08-F	84	HFD-L	430	9.11.08-R	98	HFD-H	559	12.08.08-M	110
SD	87	02.05.09-R	119	HFD	394	7.08.08-T	88	HFD-L	455	9.24.08-W	99	HFD-H	547	12.17.08-W	111
SD	101	02.05.09-R	119	HFD	333	7.11.08-F	89	HFD-L	451	9.27.08-Sa	100	HFD-H	961	12.18.08-R	112
SD	62	02.19.09-R	121	HFD	409	7.14.08-M	89	HFD-L	502	10.27.08-Sa	100	HFD-H	543	12.23.08-T	112
SD	50	02.26.09-R	122	HFD	415	7.28.08-M	91	HFD-L	421	10.02.08-R	101	HFD-H	590	12.29.08-M	113
SD	104	02.28.09-Sa	122	HFD	341	8.04.08-M	92	HFD-L	477	10.07.08-T	101	HFD-H	575	01.04.09-Su	111
SD	103	03.02.09-M	122	HFD	340	8.13.08-W	93	HFD-L	444	10.13.08-M	102	HFD-H	576	01.04.09-Su	111
SD	97	03.04.09-W	122	HFD	350	8.15.08-F	94	HFD-L	510	10.14.08-T	102	HFD-H	621	01.10.09-Sa	115
SD	948	03.07.09-Sa	123	HFD	413	8.20.08-W	94	HFD-L	482	10.16.08-R	103	HFD-H	582	01.14.09-W	115
SD	75	08.09.08-Su	123	HFD	320	8.25.08-M	95	HFD-L	471	10.30.08-R	105	HFD-H	596	01.19.09-M	116
SD	18	03.12.09-R	124	HFD	417	9.02.08-T	96	HFD-L	520	10.31.08-F	105	HFD-H	567	01.26.09-M	117
SD	29	03.12.09-R	124	HFD	317	9.05.08-F	97	HFD-L	500	11.12.08-W	106	HFD-H	572	01.28.09-W	117
SD	57	3.13.09-F	124	HFD	348	9.15.08-M	98	HFD-L	504	11.15.08-Sa	107	HFD-H	540	02.03.09-T	118
SD	39	3.16.09-M	124	HFD	356	9.15.08-M	98	HFD-L	457	11.18.08-T	107	HFD-H	544	02.04.09-W	118
SD	72	3.21.09-Sa	125	HFD	363	10.01.08-W	100	HFD-L	960	11.18.08-T	107	HFD-H	527	02.06.09-F	119
SD	43	3.23.09-M	125	HFD	337	10.02.08-R	101	HFD-L	452	11.19.08-W	107	HFD-H	529	02.08.09-Su	119
SD	45	3.25.09-W	125	HFD	376	10.31.08-F	105	HFD-L	459	11.20.08-R	108	HFD-H	620	02.10.09-T	119
SD	12	4.03.09-F	127	HFD	342	11.01.08-Sa	105	HFD-L	521	11.20.08-R	108	HFD-H	585	02.14.09-Sa	120
SD	27	4.05.09-Su	127	HFD	375	11.06.08-R	106	HFD-L	467	11.22-08-Sa	108	HFD-H	581	02.16.09-M	120
SD	47	4.05.09-Su	127	HFD	367	11.12.08-W	106	HFD-L	423	11.26.08-W	108	HFD-H	595	02.20.09-F	121
SD	58	04.10.09-F	128	HFD	316	11.20.08-R	108	HFD-L	493	11.26.08-W	108	HFD-H	537	02.21.09-Sa	121
SD	44	04.11.09-Sa	128	HFD	344	11.20.08-R	108	HFD-L	440	11.28.08-F	109	HFD-H	561	03.05.09-R	123
SD	16	4.20.09-M	129	HFD	345	11.20.08-R	108	HFD-L	454	12.03.08-W	109	HFD-H	580	03.06.09-F	123
SD	30	4.22.09-W	129	HFD	346	11.20.08-R	108	HFD-L	458	12.08.08-M	110	HFD-H	616	03.09.09-M	123
SD	79	4.22.09-W	129	HFD	352	11.21.08-F	108	HFD-L	427	12.16.08-T	111	HFD-H	627	03.12.09-R	124
SD	24	4.23.09-R	130	HFD	362	11.21.08-F	108	HFD-L	496	12.16.08-T	111	HFD-H	555	3.20.09-F	125
SD	94	4.24.09-F	130	HFD	403	11.22-08-Sa	108	HFD-L	437	12.21.08-Su	112	HFD-H	563</td		

Supplementary Table 2 | SRT1720 levels in plasma.

	Diet Treatment (<i>n</i>)		
	SD (8)	HFD-L (8)	HFD-H (8)
Morning			
(μ g/mL)	ND	0.32 ± 0.04	0.67 ± 0.08
(μ M)	ND	0.69 ± 0.09	1.46 ± 0.18
Evening			
(μ g/mL)	ND	0.45 ± 0.08	0.69 ± 0.08
(μ M)	ND	0.95 ± 0.17	1.46 ± 0.24

Values are means \pm SEM. *n*, animals per group; ND, none detected.

Supplementary Table 3a | Major pathologies at 82 weeks of age as determined by blinded histopathological analysis.

The percentage of mice developing various pathologies is represented in most cases, with glomerulonephritis representing an average score in a range of 0-4, with 4 being the most severe. Overall there was no major effect due to SRT1720 on pathology at this time point.

		Diet Treatment (<i>n</i>)			
		SD (6)	HFD (6)	HFD-L (6)	HFD-H (6)
Heart	Normal (%)	67	100	100	100
	Mild interstitial fibrosis (%)	33	0	0	0
Kidney	Glomerulonephritis (AUs)	2.1 ± 0.4	2.0 ± 0.4	1.3 ± 0.2	2.0 ± 0
	Lymphocyte infiltration (%)	83	67	83	33
	Lymphoma (%)	0	33	0	67
Liver	Normal (%)	16	0	0	0
	Congestion (%)	33	0	0	0
	Lymphocyte infiltration (%)	67	50	83	83
	Lymphoma (%)	33	33	33	33
Spleen	EMH (%)	50	83	83	83
	Congestion (%)	17	17	17	0
	Neoplasia (%)	33	17	0	33
Lung	Normal (%)	50	0	0	0
	Congestion (%)	50	100	100	100
	Edema (%)	17	0	0	0
	Lymphocyte infiltration (%)	17	33	0	17
	Neoplasia (%)	0	17	17	17

Supplementary Table 3b | Major pathologies identified at necropsy.

The percentage of mice presenting with various pathologies is represented.

		Diet Treatment (<i>n</i>)			
		SD (92)	HFD (101)	HFD-L (102)	HFD-H (95)
Heart	Enlarged	7	23	19	24
	Pericardial fat	1	10	8	3
	Ischemic foci	1	6	1	0
Kidney	Perirenal fat	0	5	2	4
Liver	Hepatocarcinoma	35	21	21	22
	Steatosis	4	43	24	11

Supplementary Table 4a | Z scores of gene pathways affected by SRT1720 treatment.

PathwayName (MSigDB)	HFD:SD	HFD-L:HFD	HFD-H:HFD
ICHIBA_GVHD	10.88	-7.67	-6.68
WIELAND_HEPATITIS_B_INDUCED	10.33	-6.84	-5.65
IGLESIAS_E2FMINUS_UP	10.14	-8.72	-6.84
AGEING_KIDNEY_UP	8.50	-9.86	-6.85
FLECHNER_KIDNEY_TRANSPLANT_REJECTION_UP	8.48	-8.08	-5.72
CARIES_PULP_UP	7.91	-7.48	-3.90
EMT_UP	7.09	-7.75	-5.92
LEE_MYC_E2F1_UP	7.02	-8.27	-3.82
JECHLINGER_EMT_UP	6.48	-7.94	-6.25
CROONQUIST_RAS_STROMA_DN	6.46	-4.21	-2.71
LAL_KO_6MO_UP	6.21	-4.49	-1.06
ADIP_HUMAN_DN	6.09	-5.82	-5.34
LEE_E2F1_UP	6.07	-9.33	-5.58
PROSTAGLANDIN_SYNTHESIS_REGULATION	5.98	-5.71	-1.05
RUTELLA_HEMATOGFSNDCS_DIFF	5.93	-5.30	-4.48
HADDAD_CD45CD7_PLUS_VS_MINUS_UP	5.93	-5.24	-3.06
HADDAD_HSC_CD7_UP	5.93	-5.24	-3.06
YAO_P4_KO_VS_WT_UP	5.89	-4.84	-0.78
TAKEDA_NUP8_HOXA9_10D_DN	5.87	-5.77	-3.60
POD1_KO_DN	5.85	-5.12	-4.93
LAL_KO_3MO_UP	5.80	-3.96	-0.18
LEE_ACOX1_UP	5.78	-9.40	-3.26
GLUTATHIONE_METABOLISM	5.66	-2.43	-0.93
CROONQUIST_IL6_STROMA_UP	5.55	-3.84	-2.57
CPR_NULL_LIVER_UP	5.42	-1.53	-0.29
TAKEDA_NUP8_HOXA9_8D_DN	5.41	-4.75	-4.40
AGEING_KIDNEY_SPECIFIC_UP	5.34	-6.71	-4.06
BRCA_ER_NEG	5.34	-7.27	-4.89
VERHAAK_AML_NPM1_MUT_VS_WT_DN	5.28	-6.02	-4.94
ZHAN_PCS_MULTIPLE_MYELOMA_SPKD	5.28	-3.06	-1.37
TAKEDA_NUP8_HOXA9_3D_UP	5.25	-3.61	-4.40
SANSOM_AP5_DN	5.22	-1.52	-1.47
NADLER_OBESITY_UP	5.09	-6.13	-3.59
YU_CMYC_DN	5.02	-2.70	-3.56
SANA_IFNG_ENDOTHELIAL_UP	5.00	-1.67	-3.47
ERM_KO_SERTOLI_DN	5.00	-2.62	-0.28
CARIES_PULP_HIGH_UP	4.94	-4.50	-1.33
KUMAR_HOXA_DIFF	4.88	-3.24	-3.66
LEE_MYC_TGFA_UP	4.86	-10.34	-4.49
SCHRAETS_MLL_UP	4.84	-4.33	-2.78
PASSERINI_EM	4.80	-5.43	-3.40

DAC_FIBRO_UP	4.77	-3.54	-2.89
TAKEDA_NUP8_HOXA9_10D_UP	4.77	-4.74	-5.40
CMV_24HRS_DN	4.73	-3.60	-2.19
LIMONENE_AND_PINENE_DEGRADATION	4.73	-1.27	-1.53
STEMCELL_COMMON_DN	4.67	-3.38	-2.71
SANA_TNFA_ENDOTHELIAL_DN	4.62	-6.54	-4.40
WANG_HOXA9_VS_MEIS1_DN	4.62	-4.37	-4.85
MIDDLEAGE_UP	4.61	-3.85	-3.53
CMV_HCMV_TIMECOURSE_24HRS_DN	4.58	-5.43	-4.24
BAF57_BT549_UP	4.55	-4.97	-3.56
ABRAHAM_MM_VS_AL_DN	4.50	-3.60	-3.58
BOQUEST_CD31PLUS_VS_CD31MINUS_UP	4.50	-6.65	-6.16
ABRAHAM_AL_VS_MM_UP	4.49	-3.37	-3.38
HUMAN_TISSUE_THYMUS	4.48	-4.67	-2.82
HOHENKIRK_MONOCYTE_DEND_UP	4.48	-4.51	-5.04
NF90_UP	4.45	-4.26	-2.68
TAKEDA_NUP8_HOXA9_8D_UP	4.44	-4.49	-4.37
BRENTANI_IMMUNE_FUNCTION	4.37	-3.59	-3.52
SANA_IFNG_ENDOTHELIAL_DN	4.36	-7.34	-6.02
GREENBAUM_E2A_DN	4.36	-4.29	-4.32
ADIP_VS_FIBRO_UP	4.33	-0.53	0.10
GOLDRATH_CYTOLYTIC	4.27	-1.99	-2.64
BRCA_PROGNOSIS_NEG	4.13	-4.84	-3.66
IFNA_HCMV_6HRS_UP	4.12	-2.92	-3.43
LI_FETAL_VS_WT_KIDNEY_UP	4.09	-3.27	-1.10
VEGF_MMMEC_ALL_UP	4.07	-5.97	-4.70
GILDEA_BLADDER_UP	4.05	-3.48	-3.52
IRITANI_ADPROX_VASC	4.05	-5.92	-4.65
NAKAJIMA_MCS_UP	4.05	-3.61	-3.46
CROONQUIST_IL6_RAS_UP	4.02	-1.38	-1.54
HOFFMANN_BIVSBII_LGBII	4.01	-3.86	-3.40
ZHAN_MULTIPLE_MYELOMA_VS_NORMAL_DN	3.96	-2.08	-0.51
VEGF_MMMEC_12HRS_UP	3.95	-4.06	-1.44
LE_MYELIN_UP	3.93	-6.30	-2.98
BROWN_GRAN_MONO_DIFFERENTIATION	3.91	-2.20	-0.06
BASSO_HCL_DIFF	3.91	-4.47	-2.95
ADIPOGENESIS_HMSC_CLASS8_DN	3.89	-3.82	-2.29
BUTANOATE_METABOLISM	3.89	-1.49	-0.14
TGFBETA_C1_UP	3.89	-4.93	-5.07
TAKEDA_NUP8_HOXA9_16D_UP	3.88	-3.25	-3.61
ALCALAY_AML_NPMC_DN	3.88	-1.36	-2.39
BRG1_SW13_UP	3.85	-5.14	-4.65
CMV_ALL_DN	3.81	-2.39	-2.49
VERHAAK_AML_NPM1_MUT_VS_WT_UP	3.79	-1.78	-2.75
BOQUEST_CD31PLUS_VS_CD31MINUS_DN	3.78	-3.02	-2.22
ROS_MOUSE_AORTA_DN	3.77	-4.99	-1.55
TGFBETA_ALL_UP	3.71	-4.63	-4.55
IDX_TSA_UP_CLUSTER6	3.71	-1.70	-0.44

RUTELLA_HEPATGFSNDCS_UP	3.70	-0.42	-1.39
DIAB_NEPH_UP	3.67	-4.72	-5.26
HOHENKIRK_MONOCYTE_DEND_DN	3.64	-3.00	-1.86
PASSERINI_SIGNAL	3.63	-3.94	-3.36
CAPROLACTAM_DEGRADATION	3.58	-1.68	-1.57
ADIP_DIFF_CLUSTER1	3.51	-3.51	-2.16
VEGF_MMMEC_6HRS_UP	3.50	-4.10	-3.50
VANTVEER_BREAST_OUTCOME_GOOD_VS_POOR_DN	3.49	-5.33	-4.35
JISON_SICKLECELL_DIFF	3.49	-4.99	-4.15
ZHAN_MMPC_PC	3.49	-2.73	-3.78
ZHAN_TONSIL_BONEMARROW	3.48	-3.64	-3.50
HEARTFAILURE_VENTRICLE_DN	3.48	-3.28	-4.78
MANALO_HYPOXIA_UP	3.46	-5.04	-4.96
TRYPTOPHAN_METABOLISM	3.41	2.95	0.54
GRANDVAUX_IRF3_UP	3.41	-2.10	-3.30
ZHAN_MMPC_SIM	3.41	-2.88	-1.74
ZHAN_MMPC_LATEVS	3.40	-3.78	-3.99
RADAЕVA_IFNA_UP	3.38	-4.00	-4.49
GUO_HEX_DN	3.38	-5.04	-5.96
IDX_TSA_DN_CLUSTER2	3.35	-4.88	-2.90
ADIP_DIFF_UP	3.35	-0.32	0.58
IRITANI_ADPROX_DN	3.34	-3.22	-3.29
ROSS_CBF_MYH	3.33	-5.57	-2.88
PROPANOATE_METABOLISM	3.33	0.38	-0.11
DAC_PANC_UP	3.29	-2.97	-2.49
MOUSE_TISSUE_KIDNEY	3.29	-0.17	-0.02
SCHURINGA_STAT5A_DN	3.24	-1.98	-3.35
VALINE_LEUCINE_AND_ISOLEUCINE_DEGRADATION	3.23	1.20	0.57
HOFFMANN_BIVSBII_BI	3.22	-5.22	-2.32
BLEO_HUMAN_LYMPH_HIGH_24HRS_UP	3.20	-2.76	-2.04
YAGI_AML_PROG_FAB	3.20	-3.69	-2.38
TAVOR_CEBP_DN	3.18	-4.02	-3.09
DNMT1_KO_DN	3.18	-2.89	-2.72
TPA_SENS_LATE_UP	3.17	-3.27	-1.78
SLRPPATHWAY	3.17	-2.27	-2.61
FATTY_ACID_METABOLISM	3.16	2.25	2.09
SARCOMAS_SYNVOIAL_DN	3.16	-1.52	-1.57
PENG_RAPAMYCIN_UP	3.14	-1.40	-1.63
ROSS_MLL_FUSION	3.14	-1.95	-0.13
LEE_TCELLS2_UP	3.11	-4.45	-3.80
TNFALPHA_ADIP_DN	3.11	0.09	1.14
GNATENKO_PLATELET	3.09	-2.81	-3.02
GNATENKO_PLATELET_UP	3.09	-2.81	-3.02
ZMPSTE24_KO_DN	3.09	1.69	1.20
TAKEDA_NUP8_HOXA9_3D_DN	3.08	-5.01	-3.96
MITOCHONDRIA	3.08	-0.58	-0.31
GAY_YY1_DN	3.07	-1.54	-0.39
BRCA1_OVEREXP_UP	3.05	-2.68	-2.03

RORIE_ES_PNET_UP	3.04	-2.15	-2.40
IFNALPHA_NL_UP	3.01	-3.83	-3.52
ZHAN_MM_CD138_CD1_VS_REST	2.98	-1.37	0.10
ROSS_AML1ETO	2.97	-3.29	-1.26
FLECHNER_KIDNEY_TRANSPLANT_REJECTION_DN	2.96	2.48	0.42
AGED_RHESUS_DN	2.96	-2.68	-2.62
KNUDSEN_PMNS_DN	2.95	-2.46	-0.90
HYPOXIA_NORMAL_UP	2.95	-3.01	-1.68
DAVIES_MGUS_MM	2.93	-5.46	-2.56
BRCA1_OVEREXP_PROSTATE_UP	2.92	-4.02	-2.46
JNK_UP	2.85	-1.67	-1.83
PLATELET_EXPRESSED	2.82	-2.10	-2.16
FATTY_ACID BIOSYNTHESIS_PATH_2	2.81	-1.02	-0.90
IDX_TSA_DN_CLUSTER1	2.79	-5.31	-2.83
HSC_LATEPROGENITORS_ADULT	2.78	-2.73	-0.83
AGED_MOUSE_CEREBELLUM_UP	2.77	-2.08	-0.54
CREB_BRAIN_8WKS_UP	2.76	-1.90	-0.28
AGEING BRAIN_UP	2.76	-3.05	-2.20
BRUNO_IL3_DN	2.74	-3.94	-3.58
SASAKI_ATL_UP	2.72	-2.97	-2.34
SASAKI_TCELL LYMPHOMA_VS_CD4_UP	2.72	-2.97	-2.34
RADMACHER_AMLNORMALKARYTYPE_SIG	2.69	-4.89	-2.82
HSC_LATEPROGENITORS_SHARED	2.69	-2.57	-0.66
UVB_NHEK3_C6	2.67	-1.71	-2.26
CMV_HCMV_TIMECOURSE_ALL_DN	2.67	-1.30	-1.17
HTERT_UP	2.65	-2.43	-2.92
YAMA_RECURRENT_HCC_UP	2.64	-3.52	-2.19
BRENTANI_DEATH	2.64	-1.54	-1.48
IRS_KO_ADIP_DN	2.63	-2.11	-2.80
HSC_LATEPROGENITORS_FETAL	2.63	-2.39	-0.55
ASTON_DEPRESSION_UP	2.60	-0.56	-0.23
TAKEDA_NUP8_HOXA9_16D_DN	2.59	-1.88	-1.00
IFN_ALPHA_UP	2.58	-2.08	-3.81
AGED_MOUSE_CORTEX_UP	2.57	-1.51	-1.90
IDX_TSA_DN_CLUSTER3	2.53	-2.10	-1.50
TSADAC_RKOSILENT_UP	2.52	-2.30	-3.83
DER_IFNA_UP	2.52	-2.17	-3.50
HDACI_COLON_BUT48HRS_UP	2.51	-1.09	-2.20
CASPASE_ACTIVITY	2.49	-0.76	-1.00
CYTOKINEPATHWAY	2.48	-0.57	-1.30
CELL_CYCLE_CHECKPOINT	2.48	-1.99	-1.08
TARTE_MATURE_PC	2.47	-4.07	-1.77
HOFFMANN_BIVSBII_IMVM	2.46	-2.90	-2.16
LEE_TCELLS3_UP	2.46	-2.66	-1.18
ALZHEIMERS_DISEASE_DN	2.44	-2.73	-2.57
BENZOATE_DEGRADATION_VIA_COA_LIGATION	2.43	-0.59	-0.73
GOLDRATH_MEMORY	2.41	-0.58	-0.10
SANA_TNFA_ENDOTHELIAL_UP	2.39	-1.91	-2.16

POD1_KO_MOST_DN	2.39	-1.43	-0.89
GPCRS_CLASS_A_RHODOPSIN_LIKE_2	2.39	-1.68	-1.94
GN_CAMP_GRANULOSA_DN	2.37	-3.56	-2.89
PASSERINI_OXIDATION	2.37	-2.65	-1.38
NI2_MOUSE_DN	2.37	-3.24	1.10
KIM_TH_CELLS_UP	2.35	-0.13	-1.01
VANASSE_BCL2_TARGETS	2.33	-2.69	-2.90
DOX_RESIST_GASTRIC_UP	2.30	-1.42	-0.86
PASSERINI_PROLIFERATION	2.29	-2.50	-2.64
HUMAN_MITODB_6_2002	2.27	-0.34	-0.13
BRENTANI_ANGIOGENESIS	2.23	-3.76	-4.16
GLUCONEOGENESIS	2.23	-0.36	-0.12
GLYCOLYSIS	2.23	-0.36	-0.12
CASPASEPATHWAY	2.21	-0.80	-1.57
HPV31_UP	2.18	0.66	0.02
FSH_OVARY_MCV152_UP	2.17	-1.05	0.94
KENNY_WNT_UP	2.17	-2.53	-1.77
HSC_MATURE_ADULT	2.14	-1.09	0.29
HEARTFAILURE_ATRIA_DN	2.14	-1.94	-2.00
GH_EXOGENOUS_ANY_UP	2.14	-0.75	-1.38
LIZUKA_G1_GR_G2	2.14	-0.75	-1.53
CPR_LOW_LIVER_UP	2.13	1.70	0.66
ATRIA_UP	2.12	-4.24	-2.49
P21_ANY_DN	2.09	-1.16	-0.77
PARK_MSWS_BOTH	2.07	-2.20	-3.11
P21_P53_ANY_DN	2.07	-0.96	-0.47
VENTRICLES_UP	2.07	-1.68	-1.91
BREAST_DUCTAL_CARCINOMA_GENES	2.06	-1.47	-0.67
SMITH_HERT_TDN	2.05	-0.72	-0.60
PRMT5_KD_UP	2.04	-3.37	-3.11
GH_EXOGENOUS_ALL_UP	2.01	-0.54	-0.92
SHEPARD_GENES_COMMON_BW_CB_MO	2.00	-1.13	-1.10
P21_EARLY_DN	1.99	-0.65	-1.03
CALCIUM_REGULATION_IN_CARDIAC_CELLS	1.99	-2.95	-2.44
CELL_ADHESION	1.97	-1.53	-2.00
CITRATE_CYCLE_TCA_CYCLE	1.96	1.61	0.71
KREBS_TCA_CYCLE	1.95	0.68	-0.20
CANCER_UNDIFFERENTIATED_META_UP	1.94	-1.79	-1.32
AGED_MOUSE_HYPOTH_UP	1.92	-2.09	-0.71
GPCRDB_CLASS_A_RHODOPSIN_LIKE2	1.90	-2.14	-2.61
AGEING_KIDNEY_SPECIFIC_DN	1.87	2.16	0.82
MYOSINPATHWAY	1.84	-0.43	-0.84
HDACI_COLON_BUT2HRS_DN	1.77	-1.75	-1.97
GO_ROS	1.77	0.05	1.38
N_GLYCANE_DEGRADATION	1.71	-0.22	0.55
DER_IFNG_UP	1.71	-1.12	-1.77
P21_P53_MIDDLE_DN	1.69	-0.44	-0.50
MOOTHA_VOXPHOS	1.68	-4.34	-2.52

ICF_UP	1.68	-2.42	-2.09
XU_ATRA_UP	1.66	-1.65	0.32
PARK_MSCS_LIN2	1.64	-0.44	-0.24
PENTOSE_AND_GLUCURONATE_INTERCONVERSIONS	1.61	-0.19	-0.66
G_PROTEIN_SIGNALING	1.61	-0.34	-0.07
BCRABL_HL60_CDNA_DN	1.58	-0.06	-0.29
ELECTRON_TRANSPORT_CHAIN	1.54	-5.18	-2.41
IFNGPATHWAY	1.50	-0.13	-0.22
KAMMINGA_EZH2_TARGETS	1.49	-1.33	-0.66
NKTPATHWAY	1.47	-1.12	-0.53
CCR5PATHWAY	1.44	-0.16	-0.79
CHEMICALPATHWAY	1.39	0.22	-0.05
HDAC1_COLON_TSA2HRS_DN	1.32	0.45	-0.95
DAC_FIBRO_DN	1.23	0.27	-0.35
ARGININECPATHWAY	1.21	1.96	0.91
TSADAC_RKOEXP_UP	1.20	-1.35	-1.72
SULFUR_METABOLISM	1.15	0.97	-0.54
STAEGE_EFTS_UP	1.11	-0.66	-0.59
GLYCOLYSISPATHWAY	0.91	-1.07	-1.47
FERRANDO_LYL1_NEIGHBORS	0.89	-1.49	-0.46
CHEOK_LDMTX_MP_UP	0.76	-1.73	-0.44
E2F1_DNA_UP	0.76	-0.73	-0.02
TSADAC_HYPERMETH_HYPERAC_OVCA_UP	-0.63	0.33	0.85
IGF1MTORPATHWAY	-0.79	0.64	0.87
TSADAC_HYPERMETH_OVCA_UP	-0.81	0.45	0.88
NGFPATHWAY	-0.87	0.89	0.80
CHEOK_MP_DN	-0.97	0.77	0.21
ST_GAQ_PATHWAY	-0.99	0.28	0.14
HUMAN_TISSUE_TESTIS	-1.07	0.87	1.03
CANTHARIDIN_UP	-1.10	0.86	1.16
ANDROGEN_AND_ESTROGEN_METABOLISM	-1.13	3.39	1.06
ST_ERK1_ERK2_MAPK_PATHWAY	-1.14	0.38	1.75
IL4PATHWAY	-1.15	1.03	0.42
INTEGRINPATHWAY	-1.22	0.24	0.91
MUNSHI_MM_VS_PCS_DN	-1.25	-0.20	-0.79
IGF1PATHWAY	-1.37	2.07	1.47
IL2PATHWAY	-1.38	1.30	1.13
BRCA2_BRCA1_UP	-1.44	0.42	0.06
MRNA_BINDING_ACTIVITY	-1.48	0.08	0.27
HOFMANN_MANTEL_LYMPHOMA_VS_LYMPH_NODES_UP	-1.54	0.12	0.75
INSULINPATHWAY	-1.55	1.79	1.36
CMV_HCMV_TIMECOURSE_20HRS_UP	-1.58	0.08	-0.43
CERAMIDEDEPATHWAY	-1.59	0.32	0.89
AKTPATHWAY	-1.59	0.74	1.35
UVB_NHEK1_C6	-1.64	1.67	0.75
CANTHARIDIN_DN	-1.66	-0.70	0.38
RANPATHWAY	-1.66	0.32	0.48
UVC_TTD_4HR_DN	-1.66	2.90	1.82

ST_TUMOR_NECROSIS_FACTOR_PATHWAY	-1.67	0.95	0.81
RNA_TRANSCRIPTION.REACTOME	-1.69	0.09	0.20
RIBOSOMAL_PROTEINS	-1.69	-7.48	-3.66
UVC_XPCS_8HR_DN	-1.74	2.52	1.21
UVB_NHEK1_DN	-1.76	1.44	1.37
INSULIN_ADIP_INSENS_UP	-1.79	2.73	3.21
ST_FAS_SIGNALING_PATHWAY	-1.82	0.42	-0.77
ET743_SARCOMA_DN	-1.83	1.48	1.13
HEARTFAILURE_ATRIA_UP	-1.87	0.65	0.23
BHATTACHARYA_ESC_UP	-1.88	-0.99	-0.63
FLECHNER_KIDNEY_TRANSPLANT_REJECTION_PBL_DN	-1.89	-0.58	0.15
BLEO_MOUSE_LYMPH_HIGH_24HRS_DN	-1.91	0.52	0.61
MMS_HUMAN_LYMPH_HIGH_24HRS_DN	-1.92	0.05	0.34
BRG1_H1299_UP	-1.96	1.32	0.50
TESTIS_EXPRESSED_GENES	-2.00	0.63	2.38
UVB_SCC_DN	-2.02	0.79	0.97
UVB_NHEK3_C3	-2.02	0.96	1.95
UVC_TTD-XPCS_COMMON_UP	-2.03	1.85	2.12
AMINOACYL_TRNA BIOSYNTHESIS	-2.04	1.32	1.20
CANCER_NEOPLASTIC_META_UP	-2.06	0.26	-0.90
COCAINE BRAIN_4WKS_UP	-2.08	1.85	3.44
EXTRINSICPATHWAY	-2.09	2.74	1.94
SANSOM_APC_LOSS5_UP	-2.15	0.52	1.82
CMV_HCMV_TIMECOURSE_18HRS_UP	-2.16	1.70	1.95
AGUIRRE_PANCREAS_CHR8	-2.17	1.58	-0.02
TNFR2PATHWAY	-2.18	2.13	1.33
EGFPATHWAY	-2.20	1.61	0.91
IL1RPATHWAY	-2.20	1.83	1.15
HDACI_COLON_CLUSTER5	-2.21	2.14	1.18
RANKLPATHWAY	-2.27	1.15	0.95
SMITH_HTERT_UP	-2.27	1.38	-1.42
N_GLYCAN_BIOSYNTHESIS	-2.28	-1.25	-0.48
PENG_LEUCINE_DN	-2.34	-0.44	-1.21
TOLLPATHWAY	-2.36	1.31	1.13
ST_G_ALPHA_I_PATHWAY	-2.38	1.03	0.65
IL6PATHWAY	-2.40	1.56	1.71
CMV_HCMV_TIMECOURSE_16HRS_UP	-2.41	0.81	0.20
UV-4NQO_FIBRO_DN	-2.45	1.32	0.97
KERATAN_SULFATE_BIOSYNTHESIS	-2.46	-0.48	-0.42
HDACI_COLON_CUR24HRS_UP	-2.46	-0.15	0.26
HDACI_COLON_TSA2HRS_UP	-2.46	1.32	3.90
TARTE_PC	-2.47	-0.88	0.46
TRANSLATION_FACTORS	-2.49	0.31	-0.13
SANSOM_APC_LOSS4_UP	-2.57	0.73	1.76
HEDVAT_ELF_UP	-2.60	-0.11	-0.14
TRNA_SYNTHETASES	-2.68	1.64	1.66
HUMAN_CD34_ENRICHED_TRANSCRIPTION_FACTORS	-2.71	0.85	1.18
CD40PATHWAY	-2.71	2.28	1.75

RNAPATHWAY	-2.75	1.62	1.22
ST_INTERLEUKIN_4_PATHWAY	-2.86	1.93	3.04
REFRACTORY_GASTRIC_UP	-2.86	-0.27	0.30
MRNA_PROCESSING.REACTOME	-2.91	0.18	0.80
KIM_TH_CELLS_DN	-2.93	2.14	4.13
NFKBPATHWAY	-2.94	1.23	1.11
OVARIAN_INFERTILITY_GENES	-2.99	0.51	0.42
BRCA1_OVEREXP_DN	-3.08	1.34	1.91
PENG GLUTAMINE_DN	-3.18	-1.37	-1.07
CMV_HCMV_TIMECOURSE_14HRS_UP	-3.21	1.03	0.90
PENG_RAPAMYCIN_DN	-3.26	0.28	-0.63
ALTERNATIVEPATHWAY	-3.65	3.08	0.26
IDX_TSA_UP_CLUSTER1	-3.76	5.23	9.07
BREAST_CANCER_ESTROGEN_SIGNALING	-3.90	-0.24	-1.21
SHEPARD_CRASH_AND_BURN_MUT_VS_WT_UP	-3.98	0.35	0.88
CMV_HCMV_TIMECOURSE_ALL_UP	-4.18	1.11	0.53
MARCIENIAK_CHOP_DIFF	-4.22	-0.62	-0.47
AS3_FIBRO_DN	-4.47	-0.51	-2.03
ADIP_DIFF_CLUSTER2	-5.08	4.19	5.83
CHEN_HOXA5_TARGETS_UP	-5.12	3.53	2.67

Supplementary Table 4b | Primer sequences used for real-time RT-PCR.

Name	Accession #	Sequence	5' position	Target Length
β-actin s	NM_007393	AATAAGTGGTTACAGGAAGTC	1548	169
β-actin as	NM_007393	ATGAAGTATTAAGGCGGAAG	1716	169
Cish s	NM_009895.3	CTCGTCCTCCAAGCTGTC	171	116
Cish as	NM_009895.3	GGGATGGAAGGAGAAAGGAG	287	116
Cyp17a1 s	NM_007809.3	TGGTCATATGCATGCCACT	295	131
Cyp17a1 as	NM_007809.3	CCCTTCTTCACGAGCACTTC	426	131
Cyp1a2 s	NM_009993.3	AATGTACCTCAGGGAATGC	741	126
Cyp1a2 as	NM_009993.3	GCTCCTGGACAGTTTCTGC	867	126
eNOS s	NM_008713	ACTGCTAGAGGTGCTGGAG	2748	112
eNOS as	NM_008713	GCTGGGTGCTGAAGTGAC	2859	112
Foxq1 s	NM_008239.4	GGCAACTGATGACAGCAGAA	987	121
Foxq1 as	NM_008239.4	TGTAGGAGTATGGGGCTTG	1108	121
Gadd45g s	NM_011817.1	TGCCTTGGAGAAGCTCAGTT	492	118
Gadd45g as	NM_011817.1	TCACCAAGTCGATCAGACCA	610	118
Hes1 s	NM_008235.2	ACACCGGACAAACCAAAGAC	304	146
Hes1 as	NM_008235.2	ATGCCGGGAGCTATCTTCT	450	146
HPRT s	NM_013556	TGCTGCGTCCCCAGACTTTG	956	76
HPRT as	NM_013556	AGATAAGCGACAATCTACCAGAGG	1031	76
ICAM1 s	NM_010493	TTCACCAGTCACATAAACACT	2255	227
ICAM1 as	NM_010493	CTTGCA CGACCC TTCTA	2481	227
Igfbp5 s	NM_010518.2	GACCCCGGAAATGTATTCT	1724	103
Igfbp5 as	NM_010518.2	CCAACGTTGCTTCTTC	1827	103
IL 1 s	NM_008361	TCTATACCTGTCTGTGAATG	617	194
IL 1 as	NM_008361	GCTTGTGCTCTGTTGT	810	194
IL 6 s	NM_031168	TCCATCCAGTTGCCCTCTG	57	175
IL 6 as	NM_031168	TTTCTCATTCACGATTCCC	231	175
iNOS s	NM_010927	TCCTACACCAACACAAAC	2548	199
iNOS as	NM_010927	CTCCAATCTGCCATCC	2746	199
Lyve1 s	NM_053247.4	TCAGAGACAGGCTTCAGGT	1304	134
Lyve1 as	NM_053247.4	TACATGTGCCCTGGTCCAAA	1438	134
PIk3 s	NM_013807.2	ACCTACAGCACCGCCATATC	438	136
PIk3 as	NM_013807.2	CTCTGGTTCCAACAGGGTGT	574	136
Sox18 s	NM_009236.2	TTTCCAATCCTGTGTCACC	975	110
Sox18 as	NM_009236.2	CTGGTCAAATT CGGTGAGGT	1085	110
TNF s	NM_013693	GCACCACCATCAAGGACTC	1078	148
TNF as	NM_013693	AGGTCTGAAGGTAGGAAGGC	1225	148
UBC s	NM_019639	TGACAGGCAAGACCATCAC	2,531	125
UBC as	NM_019639	CCAAGAACAGCACAGGAG	2,655	125
YWHAZ s	NM_011740	ACTGTCTTGTACCAACCATT	2,526	143
YWHAZ as	NM_011740	GGGCTGTAGAGAGGATGAGG	2,668	143

Supplementary Table 4c | Validation of microarray results by RT-PCR.

RNA from all animals in each group was pooled and amplified using primers specific for the indicated targets. *M* denotes fold changes obtained from the microarray analysis while *PCR* denotes values obtained by RT-PCR.

		Fold Change		
		HFD vs SD	HFD-L vs HFD	HFD-H vs HFD
Cish	<i>M</i>	-4.08	2.51	3.32
	<i>PCR</i>	2.28	6.22	3.10
Cyp17a1	<i>M</i>	3.03	-3.21	-2.47
	<i>PCR</i>	13.00	-5.06	-2.08
Cyp1a2	<i>M</i>	-1.06	2.75	3.79
	<i>PCR</i>	2.71	9.78	5.50
Foxq1	<i>M</i>	-3.57	2.56	3.20
	<i>PCR</i>	3.94	4.82	5.14
Gadd45g	<i>M</i>	-8.42	6.03	4.15
	<i>PCR</i>	-2.28	3.22	1.05
Hes1	<i>M</i>	-1.45	-1.59	-2.16
	<i>PCR</i>	-4.37	-7.27	-13.79
Igfbp5	<i>M</i>	2.87	-1.84	-2.08
	<i>PCR</i>	1.36	-1.42	-1.43
Lyve1	<i>M</i>	4.83	-2.92	-2.67
	<i>PCR</i>	1.95	-1.48	-1.81
Plk3	<i>M</i>	-2.18	2.60	4.39
	<i>PCR</i>	-3.79	1.27	1.34
Sox18	<i>M</i>	2.74	-1.97	-2.49
	<i>PCR</i>	7.25	-3.73	-1.81

Supplementary Table 4d | Genes affected by Sirt1 in liver.

HFD + SRT1720 (average of both doses) vs HFD				
<u>Array Symbol</u>	<u>Z score</u>	<u>Fold change</u>	<u>p</u>	
<i>Per reference 6.</i>				
<u>in vivo decrease:</u>				
<i>Ppary</i> **	N/A	N/A	-0.40 *	0.0480 *
<i>Per reference 7.</i>				
<u>in vivo increase:</u>				
<i>Ppara</i>	<i>Ppara</i>	0.5851864	1.08	0.5046
<i>Adipor2</i>	<i>Adipor2</i>	1.1517994	1.09	0.0007
<u>Stimulated hepatocytes increase:</u>				
<i>G6pc</i>	<i>G6pc</i>	3.4119944	1.49	0.0246
<i>Pck1</i>	<i>Pck1</i>	2.4772187	1.27	0.1486
<i>Igfbp1</i>	<i>Igfbp1</i>	3.0850113	1.45	0.0474
<i>Fgf21</i>	<i>Fgf21</i>	-1.58851	-1.16	0.3170
<i>Per reference 8.</i>				
<u>in vivo increase:</u>				
<i>Srebp-</i>				
<i>1c</i>	<i>Srebf1</i>	-1.40882	-1.19	0.0122
<i>MnSOD</i>	<i>Sod2</i>	0.3312286	-1.00	0.3727
<i>Nrf1</i>	<i>Nrf1</i>	0.4014570	1.06	0.2064
<u>in vivo decrease:</u>				
<i>IL-6</i>	N/A	N/A	-1.75 *	0.2281 *
<i>Tnfα</i>	N/A	N/A	-2.63 *	0.0119 *
<i>Per reference 9.</i>				
<u>in vivo increase:</u>				
<i>MnSOD</i>	<i>Sod2</i>	0.3312286	-1.00	0.3727
<u>in vivo decrease:</u>				
<i>IL-6</i>	N/A	N/A	-1.75 *	0.2281 *
<i>Tnfα</i>	N/A	N/A	-2.63 *	0.0119 *

* Based on RT-PCR

** HFD-H vs HFD

Supplementary Table 4e | Serum inflammatory markers.

		Serum Levels		
		SD	HFD	HFD-H
TNF-α	41 wks	5.3 ± 0.5	7.4 ± 1.9	2.9 ± 0.4
	(pg/mL)			
IL-6	41 wks	22.6 ± 5.1	35.3 ± 2.4*	13.5 ± 1.5†
	72 wks	11.7 ± 2.5	18.2 ± 2.1	7.7 ± 1.9†
MCP-1	41 wks	87.7 ± 10.7	89.9 ± 24.6	48.0 ± 6.0
	72 wks	53.6 ± 11.4	51.9 ± 12.6	43.5 ± 14.9
Leptin	41 wks	31.2 ± 6.5	51.8 ± 4.3	50.8 ± 6.1
	72 wks	29.7 ± 6.2	46.7 ± 7.0	35.5 ± 5.8

* Significant from SD

† Significant from HFD

Values are means ± SEM, n = 5-8 per group.

Supplementary Table 4f | Genes upregulated by SRT1720 and/or resveratrol in liver.

The table lists genes for which expression was increased in four comparisons (red cells), increased in three comparisons (orange cells), or increased in two comparisons (yellow cells). Values in the table list the fold-change estimate associated with each transcript, i.e., expression in the experimental treatment relative to the control. P-values listed in parentheses were obtained from the Z-ratio test procedure as previously described². The value "NS" is used to indicate transcripts for which the experimental treatment had no significant effect on gene expression ($P > 0.05$).

Illumina Ids	Symbol	SRT1720 / Control (P-Value) 30 mg/kg	SRT1720 / Control (P-Value) 100 mg/kg	Resveratrol / Control (P-value) Dose: Hi	Resveratrol / Control (P-Value) Dose: Low
ILMN_2714031	1300002F13Rik	2.13 (< 0.001)	2.15 (< 0.001)	1.68 (0.0038)	1.68 (0.002)
ILMN_2758803	1700019G17Rik	1.33 (0.0041)	1.2 (0.03)	1.28 (3.4e-07)	1.45 (< 0.001)
ILMN_1248507	Cml2	1.48 (< 0.001)	1.33 (0.034)	1.29 (1.2e-05)	1.51 (8.3e-10)
ILMN_2739847	Cyp1a2	2.75 (< 0.001)	3.79 (< 0.001)	1.36 (0.00013)	1.41 (0.0082)
ILMN_1214634	Aqp9	1.24 (0.0019)	1.25 (< 0.001)	1.11 (0.0022)	NS
ILMN_2627733	1200006F02Rik	1.25 (5e-04)	1.53 (< 0.001)	NS	1.27 (0.032)
ILMN_2659143	Hc	1.32 (< 0.001)	1.29 (4e-04)	NS	1.38 (0.04)
ILMN_1237723	Lrp1	1.22 (< 0.001)	1.26 (0.0078)	NS	1.21 (0.013)
ILMN_1216597	Slc25a25	2.85 (< 0.001)	3.12 (< 0.001)	NS	1.55 (1.9e-05)
ILMN_2619574	Slc35e3	1.48 (< 0.001)	1.22 (2e-04)	NS	1.19 (0.026)
ILMN_1247220	Tbx3	1.94 (5e-04)	1.36 (0.0021)	NS	1.22 (0.01)
ILMN_1236727	C730031G17	1.46 (< 0.001)	1.4 (8e-04)	NS	-1.29 (0.034)
ILMN_2763459	E130107N23Rik	1.29 (< 0.001)	1.27 (< 0.001)	NS	-1.41 (0.023)
ILMN_1213805	C8a	1.28 (0.03)	NS	1.69 (0.0094)	1.87 (2e-05)
ILMN_2620326	Cyp27a1	1.25 (4e-04)	NS	1.22 (0.00046)	1.28 (0.035)
ILMN_1231625	Cyp4f14	1.25 (0.032)	NS	1.34 (2e-04)	1.32 (0.00085)
ILMN_2601215	Cyp7b1	1.67 (0.0035)	NS	1.81 (0.012)	2.24 (4.4e-12)
ILMN_1254721	EG13909	1.4 (7e-04)	NS	1.35 (0.012)	1.59 (2e-05)
ILMN_2592166	Mup4	2.28 (0.043)	NS	2.22 (0.0034)	3.27 (1.5e-07)
ILMN_1237830	1110020G09Rik	1.33 (1e-04)	1.22 (0.0043)	NS	NS
ILMN_2771441	4932414K18Rik	1.25 (< 0.001)	1.23 (0.0067)	NS	NS
ILMN_2588055	Actb	1.8 (< 0.001)	1.71 (0.0094)	NS	NS
ILMN_2746475	Al788959	1.2 (< 0.001)	1.29 (< 0.001)	NS	NS
ILMN_2619565	Akr1c6	1.42 (< 0.001)	1.29 (0.018)	NS	NS
ILMN_2636403	Axud1	1.61 (0.0013)	1.5 (9e-04)	NS	NS
ILMN_1213483	B430214A04Rik	1.35 (3e-04)	1.64 (< 0.001)	NS	NS
ILMN_1220520	C730027J19Rik	1.21 (0.0013)	1.21 (0.016)	NS	NS
ILMN_1228850	Ccnl1	1.33 (0.025)	1.31 (8e-04)	NS	NS
ILMN_2764136	Cdh2	1.27 (0.0044)	1.34 (< 0.001)	NS	NS
ILMN_2718330	Cish	2.51 (< 0.001)	3.32 (0.0013)	NS	NS
ILMN_1254540	Crbn	1.26 (0.0058)	1.24 (0.001)	NS	NS
ILMN_1245217	Cyp2c50	1.6 (< 0.001)	1.39 (0.0011)	NS	NS
ILMN_1253563	Cyp2d13	1.44 (1e-04)	1.25 (0.0045)	NS	NS
ILMN_2753183	Cyp3a11	1.22 (9e-04)	1.22 (0.011)	NS	NS

ILMN_1244991	Fbxo21	1.56 (0.02)	1.46 (5e-04)	NS	NS
ILMN_1224637	Foxq1	2.56 (0.0019)	3.2 (< 0.001)	NS	NS
ILMN_1236958	Gabarapl1	1.26 (0.035)	1.2 (< 0.001)	NS	NS
ILMN_2644496	Glul	1.33 (0.036)	1.6 (< 0.001)	NS	NS
ILMN_1238680	Gopc	1.28 (0.014)	1.29 (0.0095)	NS	NS
ILMN_2737940	Grtp1	1.29 (< 0.001)	1.39 (0.0063)	NS	NS
ILMN_2718157	Impa1	1.23 (< 0.001)	1.26 (< 0.001)	NS	NS
ILMN_2723920	Itpk1	1.4 (0.0012)	1.22 (0.039)	NS	NS
ILMN_2669869	Lin7c	1.25 (0.0014)	1.36 (< 0.001)	NS	NS
ILMN_2696026	Npr2	1.63 (< 0.001)	1.29 (< 0.001)	NS	NS
ILMN_1253709	Nudt7	1.92 (< 0.001)	1.55 (0.018)	NS	NS
ILMN_2716085	Pex6	1.22 (< 0.001)	1.25 (4e-04)	NS	NS
ILMN_2623216	Pgrmc1	1.2 (< 0.001)	1.19 (0.028)	NS	NS
ILMN_2636536	Pla2g12a	1.43 (6e-04)	1.82 (3e-04)	NS	NS
ILMN_1247753	Ppap2b	1.27 (1e-04)	1.34 (4e-04)	NS	NS
ILMN_2630993	Ppap2b	1.29 (< 0.001)	1.28 (< 0.001)	NS	NS
ILMN_2665545	Rin3	1.3 (0.016)	1.33 (< 0.001)	NS	NS
ILMN_1235657	Rnase4	1.48 (0.008)	1.47 (0.013)	NS	NS
ILMN_2764143	Scap	1.27 (0.014)	1.23 (0.022)	NS	NS
ILMN_1235366	Slc16a2	1.23 (1e-04)	1.23 (< 0.001)	NS	NS
ILMN_2642339	Slc1a2	1.58 (0.0073)	1.5 (0.019)	NS	NS
ILMN_1247071	Slc22a1	1.14 (3e-04)	1.32 (3e-04)	NS	NS
ILMN_1258323	Slco1a4	1.5 (0.0083)	1.47 (0.0044)	NS	NS
ILMN_1255164	Slco1b2	1.21 (< 0.001)	1.22 (0.0027)	NS	NS
ILMN_1250011	Tob1	1.42 (< 0.001)	1.33 (0.0032)	NS	NS
ILMN_1234112	Tomm70a	1.26 (0.0042)	1.31 (< 0.001)	NS	NS
ILMN_2422333	Trap1	1.19 (< 0.001)	1.29 (< 0.001)	NS	NS
ILMN_2484465	Txrnd1	1.28 (2e-04)	1.29 (< 0.001)	NS	NS
ILMN_1212975	Wdr23	1.29 (0.0013)	1.2 (< 0.001)	NS	NS
ILMN_1250815	Wsb1	1.47 (< 0.001)	1.68 (0.0044)	NS	NS
ILMN_2595026	Yod1	1.26 (0.001)	1.29 (0.013)	NS	NS
ILMN_2473374	Zdhhc9	1.29 (0.016)	1.27 (0.0029)	NS	NS
ILMN_1241970	Zfp259	1.21 (4e-04)	1.43 (< 0.001)	NS	NS
ILMN_2769991	Cyp2c29	1.19 (1e-04)	NS	1.24 (0.0014)	NS
ILMN_1230145	Acvr2b	1.3 (6e-04)	NS	NS	1.28 (0.00011)
ILMN_2601946	AL024069	1.19 (0.0016)	NS	NS	1.38 (1.3e-05)
ILMN_1249670	Cai	1.2 (0.023)	NS	NS	1.27 (0.022)
ILMN_1259182	Gpld1	1.51 (< 0.001)	NS	NS	1.15 (0.017)
ILMN_1236788	Igfbp2	2.14 (< 0.001)	NS	NS	1.68 (0.041)
ILMN_1243228	Il1rap	1.22 (< 0.001)	NS	NS	1.19 (0.032)
ILMN_2749556	Mucdhl	1.21 (< 0.001)	NS	NS	1.4 (0.023)
ILMN_1225605	Pigr	1.25 (< 0.001)	NS	NS	1.39 (0.022)
ILMN_2670022	Plekhc1	1.28 (0.0087)	NS	NS	1.26 (0.018)
ILMN_1247506	Saa4	1.21 (< 0.001)	NS	NS	1.85 (0.027)
ILMN_2769089	Serpinf2	1.17 (0.021)	NS	NS	1.61 (0.00075)
ILMN_1222970	F5	NS	1.22 (1e-04)	NS	1.18 (0.035)
ILMN_2756023	Pcsk9	NS	1.43 (0.03)	NS	1.68 (0.00065)
ILMN_2445324	Zfpm1	NS	1.27 (< 0.001)	NS	1.27 (0.0082)
ILMN_1216182	2810439F02Rik	NS	NS	1.73 (0.00062)	2.15 (3.7e-12)
ILMN_1258394	Aars	NS	NS	1.14 (0.011)	1.31 (5e-04)

ILMN_1216720	C6	NS	NS	1.78 (0.0065)	2.37 (0.00015)
ILMN_1227404	C8b	NS	NS	2.37 (0.00093)	3.1 (4.3e-07)
ILMN_2652971	Deb1	NS	NS	1.18 (0.0058)	1.26 (0.0044)
ILMN_2707043	Ebp	NS	NS	1.14 (0.0067)	1.38 (1.2e-06)
ILMN_2693922	Egfr	NS	NS	2.41 (0.012)	3.14 (3.8e-10)
ILMN_2609762	F11	NS	NS	1.43 (9.5e-05)	1.5 (3.5e-08)
ILMN_2761645	Fetub	NS	NS	1.33 (0.0019)	1.68 (0.0012)
ILMN_1244188	H6pd	NS	NS	1.34 (0.00015)	1.4 (0.00077)
ILMN_1236304	Hamp	NS	NS	1.65 (0.0054)	1.66 (0.03)
ILMN_1234449	Hsd3b5	NS	NS	10.6 (0.0043)	14.7 (4.8e-08)
ILMN_1216279	Irf6	NS	NS	1.26 (0.01)	1.4 (9.8e-05)
ILMN_1212637	Lman1	NS	NS	1.19 (1.9e-06)	1.24 (8.2e-05)
ILMN_1216142	MAp19	NS	NS	1.14 (4e-04)	1.22 (0.038)
ILMN_1238266	Mbl1	NS	NS	1.33 (1.4e-05)	1.55 (0.0011)
ILMN_2595774	Mta2	NS	NS	1.16 (0.0053)	1.15 (0.00063)
ILMN_2663374	Nr1h3	NS	NS	1.11 (0.013)	1.31 (1.5e-05)
ILMN_1215004	Osbpl9	NS	NS	1.22 (0.0036)	1.24 (0.013)
ILMN_1220234	SerpinA1e	NS	NS	5.81 (0.0011)	9.32 (2.5e-06)
ILMN_2766867	Slc22a7	NS	NS	1.19 (8e-05)	1.27 (0.00011)
ILMN_1255237	Ssr4	NS	NS	1.14 (0.0018)	1.22 (0.011)
ILMN_3162202	Tmem86b	NS	NS	1.19 (0.0014)	1.26 (0.00075)
ILMN_1227831	Trfr2	NS	NS	1.24 (7e-05)	1.51 (3.1e-06)
ILMN_2513870	Zap70	NS	NS	1.27 (3.9e-06)	1.22 (0.00039)
ILMN_1231720	Zfp385	NS	NS	1.28 (0.011)	1.28 (0.00062)

Supplementary Table 4f | Genes downregulated by SRT1720 and/or resveratrol in liver.

The table lists genes for which expression was decreased in four comparisons (red cells), decreased in three comparisons (orange cells), or decreased in two comparisons (yellow cells). Values listed in the table are ratios of gene expression in the control treatment relative to the experimental treatment. The minus sign associated with each ratio is used to indicate lower gene expression in the experimental treatment. P-values listed in parentheses were obtained from the Z-ratio test procedure as previously described². The value "NS" is used to indicate transcripts for which the experimental treatment had no significant effect on gene expression.

Illumina Ids	Symbol	SRT1720 / Control (P-Value) 30 mg/kg	SRT1720 / Control (P-Value) 100 mg/kg	Resveratrol / Control (P-value) Dose: Hi	Resveratrol / Control (P-Value) Dose: Low
ILMN_1257020	Aldh1b1	-1.67 (1e-04)	-1.45 (0.026)	-1.51 (< 0.001)	-1.72 (6.7e-09)
ILMN_2657175	Anxa2	-2.25 (< 0.001)	-1.55 (< 0.001)	-2.11 (4e-05)	-2.81 (1.8e-09)
ILMN_2680142	Anxa5	-1.69 (0.0013)	-1.41 (9e-04)	-1.68 (0.0021)	-1.87 (2.7e-05)
ILMN_2768087	Col6a1	-1.52 (0.002)	-1.56 (1e-04)	-1.28 (0.0038)	-1.32 (0.004)
ILMN_1258526	Lgals3bp	-1.31 (0.0052)	-1.38 (3e-04)	-1.4 (0.0011)	-1.48 (0.0056)
ILMN_1225204	2510004L01Rik	NS	-1.41 (4e-04)	-1.67 (2.4e-08)	-1.88 (1.9e-05)
ILMN_2672147	9130214H05Rik	NS	-1.36 (< 0.001)	-1.37 (< 0.001)	-1.36 (0.015)
ILMN_1229547	Spon2	NS	-1.56 (0.024)	-1.52 (0.0076)	-1.48 (< 0.001)
ILMN_1216493	Suclg1	NS	-1.31 (0.0032)	-1.5 (0.0081)	-1.89 (1.5e-12)
ILMN_1236758	1600023A02Rik	-1.52 (4e-04)	NS	-2 (0.00098)	-1.95 (1.5e-06)
ILMN_2592239	Dscr5	-1.4 (< 0.001)	NS	-1.24 (0.0034)	-1.31 (0.011)
ILMN_2713285	Fhl1	-1.69 (0.0068)	NS	-1.17 (0.01)	-1.23 (0.0083)
ILMN_2615035	Mgst3	-1.46 (1e-04)	NS	-1.51 (0.0066)	-1.76 (< 0.001)
ILMN_2739760	Prelp	-1.3 (0.0041)	NS	-1.22 (1.1e-10)	-1.33 (4.6e-12)
ILMN_1229161	Eng	-1.44 (0.0017)	-1.47 (0.012)	NS	-1.24 (0.039)
ILMN_2764588	Igfbp7	-1.36 (0.026)	-1.35 (0.0044)	NS	-1.44 (0.0011)
ILMN_1255416	Ly6a	-1.3 (0.041)	-1.42 (< 0.001)	NS	-1.49 (0.027)
ILMN_2741096	Timp3	-1.78 (0.0066)	-1.7 (< 0.001)	NS	-1.33 (0.0059)
ILMN_1234425	2310020H20Rik	NS	NS	-1.17 (0.011)	-1.21 (5.9e-09)
ILMN_2718217	2310057H16Rik	NS	NS	-1.33 (< 0.001)	-1.33 (0.025)
ILMN_1224855	AA175286	NS	NS	-1.48 (2.8e-07)	-1.5 (0.0093)
ILMN_2708877	AA960558	NS	NS	-1.3 (0.00054)	-1.4 (0.0033)
ILMN_2674367	Agrn	NS	NS	-1.23 (1.8e-06)	-1.3 (7.3e-06)
ILMN_1216689	Aplp2	NS	NS	-1.26 (0.005)	-1.33 (2.5e-05)
ILMN_2598201	Cox8a	NS	NS	-1.24 (0.0016)	-1.17 (0.019)
ILMN_1214531	Cyp2b13	NS	NS	-4.05 (< 0.001)	-7.12 (1.4e-14)
ILMN_2617625	Cyp2b9	NS	NS	-2.79 (0.0076)	-3.94 (< 0.001)
ILMN_2702903	Cyp2f2	NS	NS	-1.21 (0.0093)	-1.33 (3.3e-08)
ILMN_2658054	Dhrs4	NS	NS	-1.21 (0.0064)	-1.24 (< 0.001)
ILMN_1213456	Dhrs7	NS	NS	-1.34 (0.013)	-1.42 (0.0017)
ILMN_1256234	Hmgcl	NS	NS	-1.32 (< 0.001)	-1.28 (1.7e-05)
ILMN_1226528	Kctd2	NS	NS	-1.31 (1.9e-07)	-1.24 (0.0044)
ILMN_2764883	Mafg	NS	NS	-1.27 (0.0099)	-1.28 (0.019)

ILMN_2707967	Man2b1	NS	NS	-1.22 (0.0042)	-1.19 (0.0093)
ILMN_1250774	Mdm2	NS	NS	-1.15 (0.0088)	-1.23 (< 0.001)
ILMN_2699556	Msrb2	NS	NS	-1.27 (0.0061)	-1.25 (0.0035)
ILMN_2717366	Oasl1	NS	NS	-1.32 (0.0057)	-1.29 (0.024)
ILMN_2619316	Prnp	NS	NS	-1.29 (4.6e-06)	-1.24 (0.0043)
ILMN_2776056	Rassf3	NS	NS	-1.32 (0.0012)	-1.5 (0.00031)
ILMN_1212645	Slc6a13	NS	NS	-1.18 (0.0045)	-1.18 (0.01)
ILMN_2433990	Usp18	NS	NS	-1.51 (< 0.001)	-1.68 (< 0.001)
ILMN_1218627	5730437N04Rik	NS	-1.25 (0.0021)	NS	-1.23 (0.04)
ILMN_2681232	D12Ertd647e	NS	-1.35 (0.038)	NS	-1.44 (1.2e-11)
ILMN_2735350	Gdf15	NS	-1.83 (5e-04)	NS	-1.65 (0.0088)
ILMN_1216822	Insig2	NS	-1.36 (5e-04)	NS	-1.49 (1.3e-09)
ILMN_2619848	Tfrc	NS	-1.57 (< 0.001)	-1.29 (0.0017)	NS
ILMN_2648580	1500032L24Rik	-1.33 (0.013)	NS	NS	-1.18 (0.031)
ILMN_2762944	2310061N23Rik	-1.78 (< 0.001)	NS	NS	-1.64 (< 0.001)
ILMN_2647820	Apoc2	-1.26 (0.021)	NS	NS	-1.48 (8.8e-06)
ILMN_1250068	Atpif1	-1.35 (< 0.001)	NS	NS	-1.2 (0.0011)
ILMN_1236522	Cbr1	-1.52 (0.0017)	NS	NS	-1.36 (0.0045)
ILMN_1222679	Cidec	-1.72 (0.012)	NS	NS	-2.05 (0.0033)
ILMN_2647028	Copz2	-1.3 (0.029)	NS	NS	-1.25 (0.022)
ILMN_2730797	Slc25a10	-1.3 (0.042)	NS	NS	-1.56 (0.02)
ILMN_1256775	Thrsp	-2.27 (< 0.001)	NS	NS	-1.72 (< 0.001)
ILMN_2440823	Tnxb	-1.27 (2e-04)	NS	NS	-1.41 (0.0015)
ILMN_1216215	BC036718	-1.39 (< 0.001)	NS	-1.28 (0.0025)	NS
ILMN_2684667	1810035L17Rik	-1.4 (0.033)	-1.35 (< 0.001)	NS	NS
ILMN_1250771	2010316F05Rik	-1.24 (< 0.001)	-1.25 (0.035)	NS	NS
ILMN_2678637	2200001I15Rik	-1.86 (3e-04)	-1.68 (< 0.001)	NS	NS
ILMN_2693258	2310005N03Rik	-1.4 (0.0078)	-1.3 (< 0.001)	NS	NS
ILMN_2623886	A030007L17Rik	-1.3 (1e-04)	-1.36 (< 0.001)	NS	NS
ILMN_2623859	Abcc9	-1.78 (0.036)	-1.76 (0.034)	NS	NS
ILMN_1213615	Admr	-1.68 (0.0049)	-2.13 (< 0.001)	NS	NS
ILMN_2765378	Admr	-1.77 (2e-04)	-2.15 (< 0.001)	NS	NS
ILMN_1257631	Apobec1	-1.22 (0.0022)	-1.28 (1e-04)	NS	NS
ILMN_1247626	As3mt	-1.29 (< 0.001)	-1.26 (< 0.001)	NS	NS
ILMN_3162005	BC054438	-1.44 (4e-04)	-1.43 (1e-04)	NS	NS
ILMN_2776431	C1qa	-1.35 (< 0.001)	-1.27 (0.044)	NS	NS
ILMN_2619620	C1qb	-1.41 (0.0075)	-1.37 (0.03)	NS	NS